CHRIS CHAPMAN

Fundamentals of Seismic Wave Propagation

CAMBRIDGE

FUNDAMENTALS OF SEISMIC WAVE PROPAGATION:
Addenda, Errata and Revisions

CHRIS H. CHAPMAN
Schlumberger Cambridge Research

This document contains known typos and errors in *Fundamentals of Seismic Wave Propagation*, plus some useful additions and revisions. Currently it has been updated to 3 January 2008. Changes compared with the published text are indicated by coloured text — red for errata (typos and errors), green for addenda (extra material) and magenta for revisions (revised material) — or by a change bars. This document contains extra exercises and solutions which accounts for the bulk of the additional material.

- *Page 57:* **Addendum** — add an extra exercise:

Exercise 2.5 Evaluate the ray integrals (2.3.7), (2.3.8) and (2.3.12) (remaining valid for (2.3.26)) for a medium with a linear velocity function (see Section 2.5.2). Show algebraically that the ray path is an arc of a circle.

Answer: For algebraic simplicity, we shift the depth origin so it lies where $c(z)$ would be zero, i.e. the velocity-depth function is $c(z) = c'z$. The physical medium exists for $z > 0$ if $c' > 0$, and for $z < 0$ if $c' < 0$.

The travel-time integral (2.3.7) is then

$$T(p) = \oint \frac{\mathrm{d}z}{c^2 q} = \oint \frac{\mathrm{d}z}{c'z(1-(c'pz)^2)^{1/2}} = \frac{1}{2c'} \log\left(\frac{1-cq}{1+cq}\right)\Bigg|,$$

where $cq = (1-c^2p^2)^{1/2}$. Note that the logarithm is negative and decreases to zero at the turning point $z = 1/c'p$ (but the definite integral for a positive z range, is positive, of course).

The range integral (2.3.8) is

$$X(p) = \oint \frac{p\,\mathrm{d}z}{q} = \oint \frac{c'pz\,\mathrm{d}z}{(1-(c'pz)^2)^{1/2}} = -\frac{cq}{c'p}\Bigg|.$$

We can differentiate this directly to obtain the geometrical spreading (2.3.12)

$$\frac{\mathrm{d}X}{\mathrm{d}p} = \frac{1}{cc'p^2q}\Bigg|.$$

The indefinite function for the range function $-cq/c'p$ is zero at the turning point, i.e. $-cq/c'p$ is the range measured from the turning point, so the turning point does not contribute to this differential, and this expression for $\mathrm{d}X/\mathrm{d}p$ remains valid with a turning point (2.3.26) provided the turning-point limit is omitted.

Measuring the horizontal range from the turning point, where $z = 1/c'p$, we have

$$X^2(p) + z^2 = \left(\frac{cq}{c'p}\right)^2 + z^2 = \frac{1}{(c'p)^2},$$

i.e. a circle of radius $1/c'p$.

- *Pages 92, 595 and 597:* **Addendum** — add references (Fedorov, 1968 ; Silver and Jordan, 1982† ; Mehrabadi and Cowin, 1990‡).

  and add after equation (4.4.15)

  (Fedorov, 1968, pp. 14-5, mentioned the attraction of this notation but did not pursue it; Silver and Jordan, 1982, pp. 761-2, used it as a convenient isomorphism to represent moment tensors as vectors; and, Mehrabadi and Cowin, 1990, showed that $\widetilde{\mathbf{C}}$ is a second-rank tensor).

- *Page 98:* **Addendum** — after equation (4.4.54) it is useful to add the text:

  For some purposes when using the Voigt notation for the compliances, some authors, e.g. Nye (1957, p. 134), have found it convenient to introduce factors of 2 ($S_{mn} = 2s_{ijkl}$ when either m or n is 4, 5 or 6) or 4 ($S_{mn} = 4s_{ijkl}$ when both m and n are 4, 5 or 6) rather than using the modified form, $\widetilde{\mathbf{C}}$ and $\widetilde{\mathbf{S}}$, of the matrices.

- *Page 121:* **Erratum** — the reference to Backus and Mulcahy (1976a) should be to Backus and Mulcahy (1976 b).

- *Page 124:* **Addendum** — to clarify add after the first sentence:

  Remember that the decomposition into SV and SH waves, (4.6.19) and (4.6.20), depends on the vertical axis, i.e. (4.5.80) and (4.5.81). If the axes are rotated, the decomposition will be inappropriate. The appropriate shear polarization or linear combination of expressions (4.6.19) and (4.6.20) should be used. This, of course, also applies to Sections *4.6.2.2* and *4.6.2.3*.

- *Page 133:* **Addendum** — add an extra exercise:

  Exercise 4.13 Determine the compliance matrix $\mathbf{S}$ for a TIV medium, i.e. the equivalent of (4.4.54) from (4.4.53) for isotropic media, but for (4.4.60) for TIV media (see Nye, 1957).

  Answer: Isotropic Media: In isotropic media, the Voigt matrix has

† Silver, P.G. and Jordan, T.H., 1982. Optimal estimation of scalar seismic moment, *Geophys. J.R. astr. Soc.*, **70**, 755–87.

‡ Mehrabadi, M.M. and Cowin, S.C., 1990. Eigentensors of linear anisotropic elastic materials, *Q. J. Mech. appl. Math.*, **43**, 15–41.

the form (4.4.53)

$$\mathbf{C} = \begin{pmatrix} \lambda+2\mu & \lambda & \lambda & 0 & 0 & 0 \\ \lambda & \lambda+2\mu & \lambda & 0 & 0 & 0 \\ \lambda & \lambda & \lambda+2\mu & 0 & 0 & 0 \\ 0 & 0 & 0 & \mu & 0 & 0 \\ 0 & 0 & 0 & 0 & \mu & 0 \\ 0 & 0 & 0 & 0 & 0 & \mu \end{pmatrix},$$

and the compliance matrix has the same symmetries (4.4.54). As is well known, the elastic stiffnesses can be written (4.4.49)

$$c_{ijkl} = \lambda\,\delta_{ij}\,\delta_{kl} + \mu(\delta_{ik}\,\delta_{jl} + \delta_{il}\,\delta_{jk}),$$

and the compliances as

$$s_{ijkl} = \bar{\lambda}\,\delta_{ij}\,\delta_{kl} + \bar{\mu}(\delta_{ik}\,\delta_{jl} + \delta_{il}\,\delta_{jk}),$$

where (4.4.54)

$$\begin{aligned} \bar{\lambda} &= -\frac{\lambda}{2\mu(3\lambda+2\mu)} \\ \bar{\mu} &= \frac{1}{4\mu}. \end{aligned}$$

It is readily verified that

$$\bar{\lambda} + 2\bar{\mu} = \frac{\lambda+\mu}{\mu(3\lambda+2\mu)}.$$

TIV Media: In TIV media, the Voigt matrix has the form (4.4.60)

$$\mathbf{C} = \begin{pmatrix} \lambda_\perp+2\mu_\perp & \lambda_\perp & \nu & 0 & 0 & 0 \\ \lambda_\perp & \lambda_\perp+2\mu_\perp & \nu & 0 & 0 & 0 \\ \nu & \nu & \lambda_\parallel+2\mu_\parallel & 0 & 0 & 0 \\ 0 & 0 & 0 & \mu_\parallel & 0 & 0 \\ 0 & 0 & 0 & 0 & \mu_\parallel & 0 \\ 0 & 0 & 0 & 0 & 0 & \mu_\perp \end{pmatrix},$$

and the compliance matrix must have the same symmetries with five parameters, $\bar{\lambda}_\perp$, $\bar{\mu}_\perp$, $\bar{\lambda}_\parallel$, $\bar{\mu}_\parallel$ and $\bar{\nu}$. Nye (1957, p. 147) has given expressions for the relationships between the compliances and stiffnesses. The results are (remembering that Nye (1957, p. 134) has introduced factors of 2 and 4 in the compliance terms to make the relationship between compliance and stiffness, and *vice versa*, symmetrical)

$$\bar{\lambda}_\perp = \frac{\lambda_\parallel+2\mu_\parallel}{2c} - \frac{1}{4\mu_\perp}$$

$$\begin{aligned}
\bar{\mu}_\perp &= \frac{1}{4\mu_\perp} \\
\bar{\lambda}_\parallel &= \frac{2(\lambda_\perp + \mu_\perp)}{c} - \frac{1}{2\mu_\parallel} \\
\bar{\mu}_\parallel &= \frac{1}{4\mu_\parallel} \\
\bar{\nu} &= -\frac{\nu}{c},
\end{aligned}$$

where

$$c = 2(\lambda_\parallel + 2\mu_\parallel)(\lambda_\perp + \mu_\perp) - 2\nu^2.$$

It is straightforward to confirm that this reduces to the isotropic result, in particular that $\bar{\lambda}_\perp = \bar{\lambda}_\parallel = \bar{\nu} = \bar{\lambda}$.

- *Page 154:* **Erratum** — there is a typo in the subscript in equation (5.2.41) which should read

$$\mathbf{P}_{px}(T_0, T) = -\mathbf{P}^{\mathrm{T}}_{px}(T, T_0). \tag{5.2.41}$$

- *Page 165:* **Erratum** — the factor of 1/2 is missing from the second expression in equation (5.3.18), i.e. it should read

$$\boxed{H_I(\mathbf{x}, \mathbf{p}) = \frac{1}{2}\, p_j p_k \hat{\mathbf{g}}_I^{\mathrm{T}} \mathbf{a}_{jk} \hat{\mathbf{g}}_I = \frac{1}{2}\, \hat{\mathbf{g}}_I^{\mathrm{T}} \mathbf{\Gamma} \hat{\mathbf{g}}_I} \tag{5.3.18}$$

(with no summation over I).

- *Page 166:* **Addendum** — in the parentheses after equation (5.3.20) add the sentence:

(.... Only the symmetric part of $\mathbf{a}_{jk}$ contributes to the Hamiltonian (5.3.18) and equations (5.3.20) and (5.3.21), i.e. $\mathbf{a}^S_{jk} = (\mathbf{a}_{jk} + \mathbf{a}_{kj})/2$, but (5.3.20) is valid, as $(\hat{\mathbf{g}}_I^{\mathrm{T}} \mathbf{a}_{jk} \hat{\mathbf{g}}_I)^{\mathrm{T}} = \hat{\mathbf{g}}_I^{\mathrm{T}} \mathbf{a}_{kj} \hat{\mathbf{g}}_I$).

- *Page 184:* **Erratum** — equation (5.7.9) should read

$$\alpha_{\mathsf{S}}^2\, \mathrm{d}p_{x\mathsf{S}}\, \mathrm{d}p_{y\mathsf{S}} = \sin\theta_{\mathsf{S}}\, \cos\theta_{\mathsf{S}}\, \mathrm{d}\theta_{\mathsf{S}}\, \mathrm{d}\phi_{\mathsf{S}}. \tag{5.7.9}$$

The error does not persist and equation (5.7.10) is correct.

- *Page 187–8* **Erratum** — in equations (5.7.29) and (5.7.41), the subscript x_i should be x_1, i.e.

$$\frac{\partial\,(\Delta x_1)}{\partial p_1} = \frac{A_{66}}{A_{44}^2 p_3^3}\,\Delta x_3 = \frac{\Delta x_1}{p_1}\left(1 + \frac{p_1}{p_3}\,\frac{\Delta x_1}{\Delta x_3}\right), \tag{5.7.29}$$

and

$$\begin{aligned}\frac{\partial\,(\Delta x_1)}{\partial p_1} &= \frac{\Delta x_1}{p_1}\left(1 + \frac{p_1}{p_3}\,\frac{\Delta x_1}{\Delta x_3}\right)\\ &\quad + \frac{4}{p_3 \Delta x_3}\,\frac{A_{11}A_{44}p_1^2\Delta x_3^2 - A p_1 p_3 \Delta x_1 \Delta x_3 + A_{33}A_{44}p_3^2\Delta x_1^2}{A p_1^2 + 2A_{33}A_{44}p_3^2 - A_{33} - A_{44}}.\end{aligned} \tag{5.7.41}$$

- *Page 197:* **Addendum** — add an extra exercise:

Exercise 5.12 Show that the kinematic ray equations in general anisotropic media, (5.3.20) and (5.3.21), can be rewritten (Zhu, Gray and Wang, 2005)

$$\begin{aligned}\frac{\mathrm{d}\mathbf{x}}{\mathrm{d}T} &= \mathbf{V}\\ \frac{\mathrm{d}\mathbf{p}}{\mathrm{d}T} &= -\nabla \ln c.\end{aligned}$$

Answer: In a recent abstract, Zhu, Gray and Wang (2005)† have developed an alternative expression for the kinematic ray equations in anisotropic media. Apart from being a simpler, more elegant and unifying expression, it clarifies the dependence of the equations on the appropriate parameters, and in media where the Christoffel equation can be solved analytically, simplifies computations.

The kinematic ray equations (5.3.20) and (5.3.21) are

$$\begin{aligned}\frac{\mathrm{d}x_i}{\mathrm{d}T} &= \frac{\partial H}{\partial p_i}\\ \frac{\mathrm{d}p_i}{\mathrm{d}T} &= -\frac{\partial H}{\partial x_i},\end{aligned}$$

where the Hamiltonian is given by (5.3.18)

$$H(\mathbf{x},\mathbf{p}) = \frac{1}{2}\,a_{ijkl}p_i p_k \hat{g}_j \hat{g}_l.$$

† Zhu, T., Gray, S. and Wang, D., 2005. Kinematic and dynamic raytracing in anisotropic media: theory and application, *SEG extended abstract*, **ANI 1.1**, 96–9.

The first equation is, of course, the definition of the ray (group) velocity (5.3.23)

$$V_i = \frac{\partial H}{\partial p_i} = a_{ijkl} p_k \hat{g}_j \hat{g}_l,$$

but the second kinematic ray equation involves spatial derivatives of the density normalized elastic parameters, a_{ijkl} (5.3.21). But the Hamiltonian and its spatial derivative are homogeneous of degree 2 in the slowness, i.e.

$$\begin{aligned} H(\mathbf{x}, \mathbf{p}) &= \frac{1}{c^2(\mathbf{x}, \hat{\mathbf{p}})} H(\mathbf{x}, \hat{\mathbf{p}}) \\ \frac{\partial}{\partial x_i} H(\mathbf{x}, \mathbf{p}) &= \frac{1}{2} \frac{\partial a_{ijkl}}{\partial x_i} p_j p_m \hat{g}_k \hat{g}_l = \frac{1}{c^2(\mathbf{x}, \hat{\mathbf{p}})} \frac{\partial}{\partial x_i} H(\mathbf{x}, \hat{\mathbf{p}}). \end{aligned}$$

As we have (5.3.19)

$$H(\mathbf{x}, \mathbf{p}) = \frac{1}{2},$$

on the ray, we can combine these equations to give

$$\frac{\partial}{\partial x_i} H(\mathbf{x}, \mathbf{p}) = \frac{1}{c} \frac{\partial c}{\partial x_i}.$$

Thus the kinematic ray equations can be written

$$\begin{aligned} \frac{\mathrm{d}\mathbf{x}}{\mathrm{d}T} &= \mathbf{V} \\ \frac{\mathrm{d}\mathbf{p}}{\mathrm{d}T} &= -\nabla \ln c. \end{aligned}$$

These equations are completely analogous to the acoustic equations (5.1.14) and (5.1.15). Note that the spatial derivatives of the phase velocity are calculated for fixed phase direction, $\hat{\mathbf{p}}$.

These equations are a simple, unified way to write the kinematic ray equations in anisotropic media. It appears that Zhu, Gray and Wang (2005) are the first to write the second equation as above. The equations indicate that the kinematic ray results only depend on the appropriate parameters — the group velocity and phase velocity of the appropriate ray type. In the original equation (5.3.21) this property is not obvious as all elastic parameters appear to contribute. This result is important in analyzing the sensitivity of travel times to media properties, i.e. in tomography. It also means that in media where the group and phase velocity can be found from simple analytic expressions, e.g. weak or normal TI media (Exercises 4.3, 4.5 and Section 5.7.1), computations are more straightforward and efficient

Finally, the above results simplify the dynamic ray equations. The matrix of the dynamic ray equations (5.2.20)

$$\mathbf{D} = \begin{pmatrix} \mathbf{T}^{\mathrm{T}} & \mathbf{R} \\ -\mathbf{S} & -\mathbf{T} \end{pmatrix},$$

has elements

$$\begin{aligned} T_{ij} &= \frac{\partial^2 H}{\partial x_i \partial p_j} = \frac{\partial V_j}{\partial x_i} \\ R_{ij} &= \frac{\partial^2 H}{\partial p_i \partial p_j} = \frac{\partial V_i}{\partial p_j} \\ S_{ij} &= \frac{\partial^2 H}{\partial x_i \partial x_j} = \frac{\partial^2 \ln c}{\partial x_i \partial x_j}. \end{aligned}$$

- *Page 210:* **Addendum** — Mid-page, add the paragraph:

  For some purposes such as numerical computations, it is convenient to scale the elements of the vector $\mathbf{w}$, (6.1.1) and (6.1.2), and the matrix $\mathbf{A}$, (6.3.2) and (6.3.14). Dividing the pressure of stress components in the vector $\mathbf{w}$ by a (constant) characteristic impedance, $\overline{Z} = \rho c$ say, where ρ and c are a characteristic density and velocity, all the elements of the modified vector $\mathbf{w}$ have the dimensions of (transformed) velocity and the elements of the modified matrix $\mathbf{A}$ have the dimensions of slowness. The same scaling is appropriate to unify the dimensions of the elements of the vector $\mathbf{w}$ and matrix $\mathbf{A}$ in the differential systems discussed in Chapter 7.

- *Page 217:* **Erratum** — Although the combination of equations (6.3.52) and (6.3.56) is correct, they are inconsistent with the statement in parentheses following equation (6.3.56). To make them consistent they should be modified to read

$$\boxed{\begin{aligned} W_{22} &= W_{25} = w_2 \,/\beta \\ W_{52} &= -W_{55} = -w_2 \mu \, q_\beta \,/\beta \end{aligned}} \qquad (6.3.52)$$

  and

$$w_2 = 1/(2\,\rho\; q_\beta)^{1/2}. \qquad (6.3.56)$$

- *Page 219:* **Erratum** — equation (6.3.64) has an incorrect right parenthesis in element A_{31}. The correct equation is

$$\mathbf{A} \;=\; \left(\begin{array}{ccc} 0 & 0 & -p \\ 0 & 0 & 0 \\ -pC_{13}/C_{33} & 0 & 0 \\ p^2\,(C_{11}-C_{13}^2/C_{33})-\rho & 0 & 0 \\ 0 & p^2C_{66}-\rho & 0 \\ 0 & 0 & -\rho \end{array}\right. \quad \cdots \quad \left.\begin{array}{ccc} -1/C_{44} & 0 & 0 \\ 0 & -1/C_{44} & 0 \\ 0 & 0 & -1/C_{33} \\ 0 & 0 & -pC_{13}/C_{33} \\ 0 & 0 & 0 \\ -p & 0 & 0 \end{array}\right) . \tag{6.3.64}$$

- *Page 245:* **Erratum** — the subscripts in the fraction in the final expression in equation (6.8.8) should be reversed. It should read

$$\mathbf{g}_j \to \frac{\sqrt{\mathcal{S}_j^{(\ell)}}}{\sqrt{\mathcal{S}_i^{(\ell)}}}\,\mathcal{T}_{ij}\,\mathbf{g}_i = \frac{\sqrt{(\widehat{\mathbf{V}}\cdot\hat{\mathbf{n}})_j}}{\sqrt{(\widehat{\mathbf{V}}\cdot\hat{\mathbf{n}})_i}}\,\mathcal{T}_{ij}\,\mathbf{g}_i. \tag{6.8.8}$$

Revision — with hindsight, it would have been sensible to distinguish, say with a superscript, the energy-normalized polarizations in the Green function (5.4.33)

$$\mathbf{g}^G(\mathbf{x},\mathcal{L}) = (2\rho V)^{-1/2}\hat{\mathbf{g}}, \tag{5.4.33}$$

from the energy-normalized polarizations in the plane-wave eigen-solutions (6.3.26) and (6.3.29)

$$\mathbf{g}^E(p) = (2\rho V_n)^{-1/2}\hat{\mathbf{g}}. \tag{6.3.29}$$

Equation (6.8.5) then is

$$\mathbf{g}_j^E \to \mathcal{T}_{ij}\,\mathbf{g}_i^E, \tag{6.8.5}$$

and equation (6.8.8)

$$\mathbf{g}_j^G \to \frac{\sqrt{\mathcal{S}_j^{(\ell)}}}{\sqrt{\mathcal{S}_i^{(\ell)}}}\,\mathcal{T}_{ij}\,\mathbf{g}_i^G = \frac{\sqrt{(\widehat{\mathbf{V}}\cdot\hat{\mathbf{n}})_j}}{\sqrt{(\widehat{\mathbf{V}}\cdot\hat{\mathbf{n}})_i}}\,\mathcal{T}_{ij}\,\mathbf{g}_i^G. \tag{6.8.8}$$

These are immediately equivalent noting that the expression in equation

(6.8.4)

$$\frac{\sqrt{(\rho V_n)_j}}{\sqrt{(\rho V_n)_i}}\mathcal{T}_{ij},$$

is the coefficient with respect to unit displacement.

- *Page 246 and Solutions page 77:* **Erratum** — routine `TidyEigen` given in the *Solutions of Exercises* for Exercise 6.1 contained a typo. On line 148 of the routine (line 13 on page 87 of the *Solutions of Exercises*), the variable `nCP` should have been `nCp`.
  Addendum — this exercise could useful have included *Further reading* on the subject of identifying the up- and down-going eigenvectors (Colin Thomson, personal communication). In the code given in the answers to the exercises, the routine `TidyEigen` uses the normal component of the group velocity V_n to discriminate the propagation direction of the eigenvectors. Burridge (1970, Section 5)† and van der Hijden (1987, Section 6.3) discuss an alternative method based on the analytic continuation of the slowness eigenvalues, p_n. They give detailed arguments concerning the Riemann surfaces and singularities of the function $p_n(\mathbf{p}_\perp)$ — here we just summarize the more important results using our notation.

  We assume that the coordinate system has been rotated into an interface basis, e.g. equations (6.0.1) and (6.0.2), so that the slowness component normal to the interface is $p_3 = p_n$. We consider a general cross-section of the slowness surfaces defined by an angle χ such that

$$\begin{aligned} p_1 &= \mathsf{p}\cos\chi \\ p_2 &= \mathsf{p}\sin\chi. \end{aligned}$$

  In the interfaces basis (6.0.1), $\chi = 0$ but in general we consider any real angle. Note that $\mathsf{p} = |\mathbf{p}_\perp|$ is not to be confused with $p = |\mathbf{p}|$. For fixed χ, we study the six solutions $p_3^n(\mathsf{p})$ with $n = \pm1$, ±2 and ±3. The solutions $p_3^n(\mathsf{p})$ can be found by solving the Christoffel equation (5.3.17) or the eigenvalue equation (6.3.14) (both leading to a sixth-order polynomial with six solutions). Our task is to associate the solutions with positive n with waves propagating in the positive x_3 direction, and *vice versa*.

  The positive definite, strain energy function (4.4.32) means that the cross-section of the slowness surfaces (χ fixed) consists of three nested ovals (an oval is topologically like a circle but not necessarily convex)

† Burridge, R., 1970. The directions in which Rayleigh waves may be propagated on crystals, *Q. J. Mech. Appl. Math.*, **23**, 217–24.

enclosing the origin. Note that the curves have point symmetry through the origin (as slowness terms are all second order in equation (5.3.17)). We label the curves O_j, $j = 1$, 2 and 3 in order of decreasing slowness (corresponding to the ordering used in the text for the eigenvectors $\mathbf{W}$). Note that in general, the index n of the solutions does not correspond to the index j of the oval — one oval may have multiple solutions. The curves have branch points at $\mathsf{p} = \pm\xi_m$ where $\mathrm{d}p_3/\mathrm{d}\mathsf{p} = \pm\infty$, again ordered in decreasing order with $m = 1$ to M. In the simplest cases, e.g. isotropy, the oval and branch point indices, j and m, correspond, but in general $M \geq 3$ and they do not. This is illustrate in Figure 6-I for α-quartz as used in Figure 5.8 in the main text (p. 168) where $M = 5$ (in this example $\chi = \pi/2$).

This figure was produced using the code

```
function Exercise61a
% Exercise 6.1a
% added to Addenda and Errata, 15 November 2004
% C12 corrected from c13 to c12 (note figures do not
% alter significantly), 17 May 2007
%
% slowness surfaces for trigonal alpha-quartz as used in
% Figure 5.8 (see Figure 10.2.1 in Musgrave, 1970).
% Shearer, P.M. and Chapman, C.H., 1988.
% Ray tracing in anisotropic media with a linear gradient,
% Geophys. J., 94, 575-580.
% Bechmann, R., 1958.  Elastic and piezoelectric constants
% of alpha-quartz, Phys. Rev., 110, 1060-1061.
% Musgrave (1970, p. 130 and 282, density ~ 2.67 and
% axis in Figure 10.2.1 (i) is reversed)
% Density normalized so units km^2 s^-2
%
c11 = 32.73;         % from Shearer and Chapman (1988)
c33 = 40.45;
c12 = 2.64;
c13 = 4.49;
c44 = 21.86;
c14 = -6.76;         % sign as Bechmann not Musgrave
%
quartz=struct( ...
'C11',c11,'C12',c12,'C13',c13,'C14', c14,'C15',  0,'C16',0,...
          'C22',c11,'C23',c13,'C24',-c14,'C25',  0,'C26',0,...
                    'C33',c11,'C34',   0,'C35',  0,'C36',0,...
                              'C44', c44,'C45',  0,'C46',0,...
                                        'C55',c44,'C56',c14,...
                                                  'C66',.5*(c11-c12));
%
cjk = cMatrices( quartz );
```

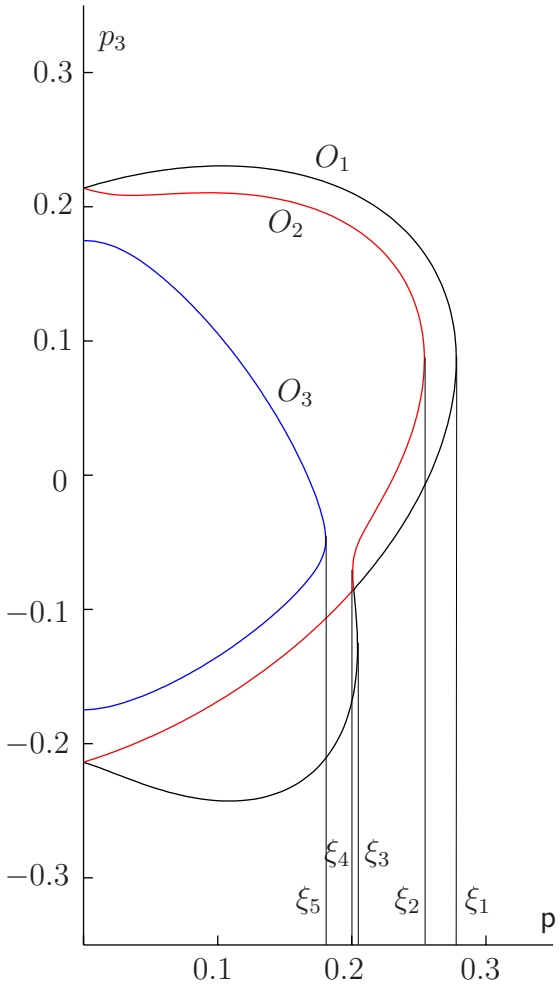

Fig. 6-I. Similar to Figure 5.8 but illustrating the branch points. The p_2 – p_3 cross-section of the three slowness surfaces O_j for α-quartz ($\chi = \pi/2$ in this cross-section) for $\mathsf{p} \geq 0$ is shown. The figure is based on the elastic constants from Bechmann (1958) as used by Shearer and Chapman (1988, p. 579). See also Figure 10.2.1(i) in Musgrave (1970). Branch points at $\mathsf{p} = \xi_m$ with $m = 1$ to 5 are indicated.

```
% modified from Exercise 5.9
for j=1:181
  theta=(j-91)*pi/180;
  ct = cos(theta);
  st = sin(theta);
  direction = [ 0 ct  st ]';     % Figure 10.2.1 (i)
%  direction = [ ct 0  st ]';     % Figure 10.2.1 (ii)
%  direction = [ ct  st 0 ]';     % Figure 10.2.1 (iii)
```

```
  [ PhaseSlow, GroupVel, Polar ] = ...
    AnisoSurfaces( direction , cjk );
  sx1(j) = ct*PhaseSlow(1);
  sz1(j) = st*PhaseSlow(1);
  sx2(j) = ct*PhaseSlow(2);
  sz2(j) = st*PhaseSlow(2);
  sx3(j) = ct*PhaseSlow(3);
  sz3(j) = st*PhaseSlow(3);
end
figure
hold on
plot( sx1, sz1, 'b' )
plot( sx2, sz2, 'r' )
plot( sx3, sz3, 'k' )
% units are km/s
axis ([0 .35 -.35 .35])
axis equal
axis manual
print -depsc2  exercise6_1a.eps
return
```

which uses the routine `AnisoSurfaces` given in the *Solutions to Exercises* for Exercise 5.9.

At a branch point, two solutions p_3^n coincide. As the product of all eigenvalues is the determinant of the matrix $\mathbf{A}$ (6.3.14), differentiating with respect to p, it is clear that for one solution $\mathrm{d}p_3^n/\mathrm{d}\mathsf{p} = +\infty$, while for the other $\mathrm{d}p_3^{-\tilde{n}}/\mathrm{d}\mathsf{p} = -\infty$ (with n and $\tilde{n}$ having the same sign), i.e. the two solutions have indices of opposite sign — near the branch point, the propagation direction has the opposite sign to the gradient — but not necessarily the same value. For $-\xi_M < \mathsf{p} < \xi_M$ between the branch points and the origin, a line p = constant must intersect each oval in two points, as there must be six solutions. At $\mathsf{p} = 0$, there will be three positive-negative pairs of solutions for $p_3(\mathsf{p})$ (from the point symmetry, or the quadratic nature of the Christoffel equation). The propagation direction is the same as the sign of the solution, i.e.

$$p_3^{-1}(0) \le p_3^{-2}(0) \le p_3^{-3}(0) < 0 < p_3^3(0) \le p_2^2(0) \le p_3^1(0).$$

Let us define

$$\bar{p}_i = p_i/\mathsf{p},$$

so $\bar{p}_1 = \cos\chi$ and $\bar{p}_2 = \sin\chi$ are real. Suppose p is positive imaginary. It is obvious that $p_3(\mathsf{p})$ cannot be purely real or imaginary but must be complex. If $\mathrm{Im}(\mathsf{p}) > 0$, then $\mathrm{Im}(\bar{\mathrm{p}}_3^{+\mathrm{n}}) < 0$ and $\mathrm{Im}(\bar{\mathrm{p}}_3^{-\mathrm{n}}) > 0$ (n positive), and *vice versa* when $\mathrm{Im}(\mathsf{p}) < 0$. $\mathrm{Im}(\bar{\mathrm{p}}_3^{\pm\mathrm{n}})$ differ in sign unless $\mathrm{Im}(\mathsf{p}) = 0$.

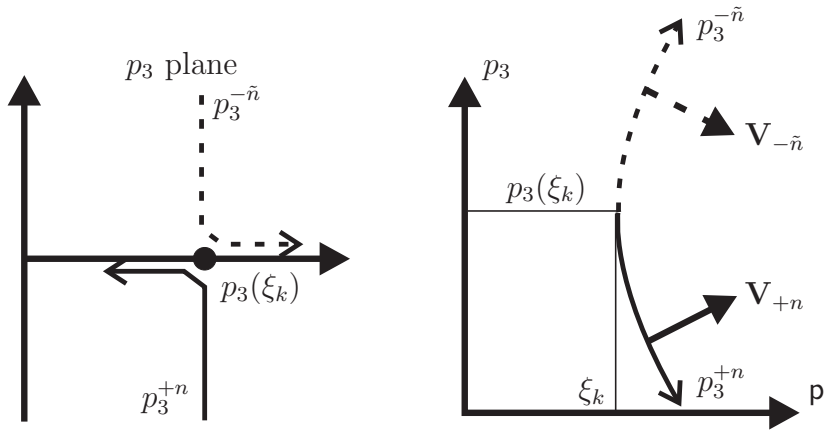

Fig. 6-II. The behaviour of the slowness $\mathbf{p}$ near a branch point: on the left, the solutions in the complex p_3 plane as p increases past a branch point at ξ_k; and on the right, the slowness surface $p_3(\mathsf{p})$ near the branch point $p_3(\mathsf{p} = \xi_k)$. In both figures, the solution propagating in the negative direction is indicated with a dashed line.

Let us consider a branch cut at $\mathsf{p} = \xi_m$ on the real axis, where two solutions p_3^{+n} and $p_3^{-\tilde{n}}$ coalesce and are real for $\mathsf{p} > \xi_k$ (n and $\tilde{n}$ are positive but not necessarily equal) as illustrated in Figure 6-II. Consider p with a small, positive imaginary part passing the branch point. For $\mathrm{Re}(\mathsf{p}) < \xi_\mathrm{k}$, $\mathrm{Im}(\mathrm{p}_3^{+\mathrm{n}}) < 0$ and $\mathrm{Im}(\mathrm{p}_3^{-\tilde{\mathrm{n}}}) > 0$. As p passes the branch point, these solutions approach the real axis at $p_3(\xi_k)$. As p passes the branch point on the left, the solutions for p_3 turn to the left. Hence $\mathrm{Re}(\mathrm{p}_3^{+\mathrm{n}}) < \mathrm{p}_3(\xi_\mathrm{k})$ and decreases, while $\mathrm{Re}(\mathrm{p}_3^{-\tilde{\mathrm{n}}}) > \mathrm{p}_3(\xi_\mathrm{k})$ and increases. As $\mathrm{d}p_3^{+n}/\mathrm{d}\mathsf{p} < 0$ it continues as the solution propagating in the positive direction, and $\mathrm{d}p_3^{-\tilde{n}}/\mathrm{d}\mathsf{p} > 0$ continues in the negative direction (as these gradients define the direction of the group velocity vector, $\mathbf{V}$). This behaviour is illustrated in Figure 6-II. A similar argument applies at branch cuts when the solutions are real for $\mathsf{p} < \xi_k$.

Burridge (1970) and van der Hijden (1987) have discussed in some detail the possible singularities of $p_3(\mathsf{p})$. Only the branch points on the real axis are significant, so we have omitted other details.

Thus as $\mathrm{Im}(\bar{\mathrm{p}}_3^{\pm\mathrm{n}})$ differ in sign unless $\mathrm{Im}(\mathsf{p}) = 0$, analytic continuity of the solutions from $\mathsf{p} = 0$ (where they are clearly identifiable), allows us to identify the solutions if $\mathrm{Im}(\mathsf{p}) \neq 0$. Taking $\mathrm{Im}(\mathsf{p}) > 0$ and small, we can identify the positive and negative propagating solutions with $\mathrm{Im}(\mathrm{p}_3^{+\mathrm{n}}) < 0$

and $\mathrm{Im}(p_3^{-\tilde{n}}) > 0$, respectively. A simple modification of the code and figure given above illustrates the algorithm. The code becomes

```
function Exercise61b
% Exercise 6.1b
% added to Addenda and Errata, 15 November 2004
% C12 corrected from c13 to c12 (note figures do not
% alter significantly), 17 May 2007
%
% illustrate algorithm for finding propagation direction
%
% slowness surfaces for trigonal alpha-quartz as used in
% Figure 5.8 (p_2 - p_3 crossection of slowness surface)
% Shearer, P.M. and Chapman, C.H., 1988.
% Ray tracing in anisotropic media with a linear gradient,
% Geophys. J., 94, 575-580.
% Bechmann, R., 1958.  Elastic and piezoelectric constants
% of alpha-quartz, Phys. Rev., 110, 1060-1061.
% Musgrave (1970, p. 130, 136 and 282, density ~ 2.67 and
% axis in Figure 10.2.1 (i) is reversed)
% Density normalized so units km^2 s^-2
%
c11 = 32.73;             % from Shearer and Chapman (1988)
c33 = 40.45;
c12 = 2.64;
c13 = 4.49;
c44 = 21.86;
c14 = -6.76;             % sign as Bechmann not Musgrave
%
quartz=struct( ...
'C11',c11,'C12',c12,'C13',c13,'C14', c14,'C15',  0,'C16',0,...
          'C22',c11,'C23',c13,'C24',-c14,'C25',  0,'C26',0,...
                    'C33',c11,'C34',   0,'C35',  0,'C36',0,...
                              'C44', c44,'C45',  0,'C46',0,...
                                        'C55',c44,'C56',c14,...
                                                  'C66',.5*(c11-c12));
%
cjk = cMatrices( quartz );
% modified from Exercise 5.9
figure
hold on
% loop over 3 slowness surfaces - blue, red and black
cols = [ 'b' 'r' 'k' ];
for n=1:3
  cnt = 0;           % point counter
  dir = +1;          % direction indicators
  % start from py = 0 which is always dir=+1
  % lots of detail to accurately pick up reversals
  for j=91:-.1:-91
    theta=(j-1)*pi/180;
```

```
    ct = cos(theta);
    st = sin(theta);
    % Figure 10.2.1 (i) in Musgrave (1970)
    direction = [ 0 ct  st ]';
    % find n-th slowness surface
    [ PhaseSlow, GroupVel, Polar ] = ...
      AnisoSurfaces( direction , cjk );
    py = ct*PhaseSlow(n);
    pz = st*PhaseSlow(n);
    % solve for p_z with slightly positive imaginary p_y
    cp = complex( py, 1.e-8 );
    [ oSlow, polarizations, tractions ] = ...
      AnisoEigen( [ 0 cp ], 1, cjk );
    [ c k ] = min(abs(oSlow-pz));
    % change  of propagation direction
    % from positive to negative direction
       if ( imag(oSlow(k)) > 0 && dir > 0 )
    % plot positive direction with solid line
      if ( cnt>0 ) plot( ppy(1:cnt), ppz(1:cnt), cols(n) ), end
      dir = -1; cnt = 1;
    % from negative to positive direction
    elseif ( imag(oSlow(k)) < 0 && dir < 0 )
    % plot negative direction with dashed line
      plot( ppy(1:cnt), ppz(1:cnt), [ cols(n) '--' ] )
      dir = +1; cnt = 1;
    % continue in same direction
    else
      cnt =cnt+1;
    end
    ppy(cnt) = py;
    ppz(cnt) = pz;
  end
  % finish
  if ( dir  > 0 )
    plot( ppy(1:cnt), ppz(1:cnt), cols(n) )
  else
    plot( ppy(1:cnt), ppz(1:cnt), [ cols(n)  '--' ] )
  end
end
% units are km/s
axis ([0 .35 -.35 .35])
axis equal
axis manual
print -depsc2  exercise6_1b.eps
return
```

which uses routines `AnisoSurfaces` from Exercise 5.9 and `AnisoEigen` from Exercise 6.1. Figure 6-III, a modification of Figure 6-I, illustrates the results, indicating the solutions propagating in a positive direction by

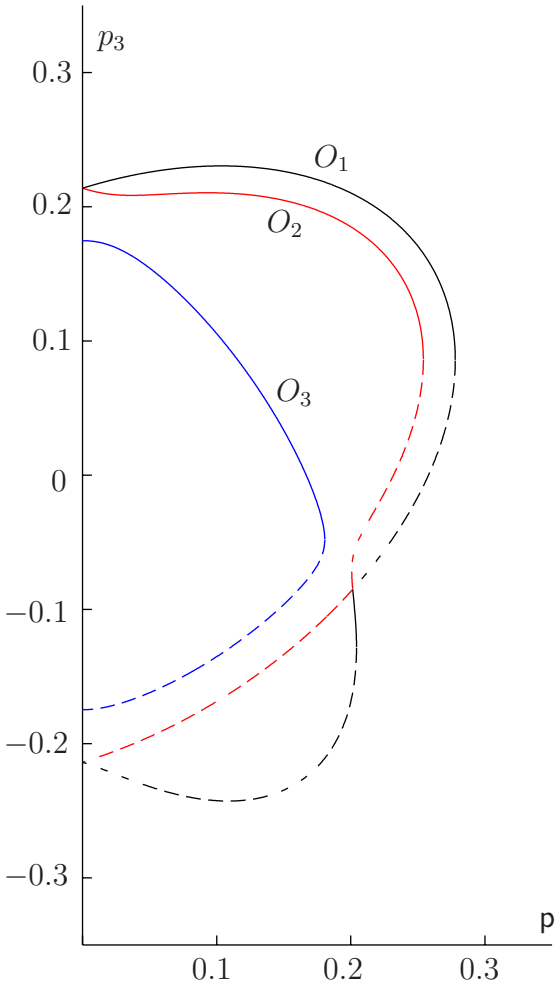

Fig. 6-III. As Figure 6-I but with the solutions propagating in a positive direction indicated by a solid line, and the solutions propagating in a negative direction by a dashed line. Note, in particular, the section with $\xi_4 < \mathsf{p} < \xi_3$ propagating in the positive direction.

solid lines, and the solutions propagating in a negative direction by dashed lines. Note, in particular, the section with $\xi_4 < \mathsf{p} < \xi_3$ propagating in the positive direction with $p_3 < 0$.

- *Page 246:* **Addendum** — add an extra exercise:

Exercise 6.4 In anisotropic media with up-down symmetry, e.g. isotropic, TIV, orthorhombic or generally monoclinic, the eigen-system (6.3.14)

must reduce to a third-order system for p_n^2, i.e. the eigenvalues of equation (6.3.14) must occur in positive-negative pairs, symmetric about the horizontal plane of symmetry. Obtain the third-order system, and demonstrate that it gives the known results for isotropic and transversely isotropic media (Section 5.7.1).

Answer:

In anisotropic elastic media with up-down symmetry, i.e. the slowness surfaces are symmetric under reflection in the horizontal plane, say the x - y plane, the eigen-system (6.3.14)

$$\mathbf{A}\mathbf{w} = p_n \mathbf{w},$$

must have some special structure. In particular, we expect the eigenvalues to be positive and negative pairs, and the equation to reduce from sixth order to a cubic in p_n^2. Up-down symmetry applies in isotropic, TIV, orthorhombic media and more generally in monoclinic anisotropic media. It is necessary to solve the eigen-system for Snell's law at interfaces, and for ray tracing in 1D media, so analyzing the structure of the equations in up-down symmetric media is important.

In monoclinic media with a horizontal, reflection symmetry plane, elastic parameters where the vertical index appears an *odd* number of times must be zero. Thus in the Voigt notation (4.4.13), the elastic parameter 6×6 matrix must be of the form

$$\mathbf{C} = \begin{pmatrix} C_{11} & C_{12} & C_{13} & 0 & 0 & C_{16} \\ C_{12} & C_{22} & C_{23} & 0 & 0 & C_{26} \\ C_{13} & C_{23} & C_{33} & 0 & 0 & C_{36} \\ 0 & 0 & 0 & C_{44} & 0 & 0 \\ 0 & 0 & 0 & 0 & C_{55} & 0 \\ C_{16} & C_{26} & C_{36} & 0 & 0 & C_{66} \end{pmatrix}.$$

Isotropic media (4.4.53) and TIV media (4.4.59) are obviously special cases of a monoclinic medium. The 3×3 stiffness matrices $\mathbf{c}_{jk}$ (4.4.39) are

$$\mathbf{c}_{11} = \begin{pmatrix} C_{11} & C_{16} & 0 \\ C_{16} & C_{66} & 0 \\ 0 & 0 & C_{55} \end{pmatrix} \quad \mathbf{c}_{22} = \begin{pmatrix} C_{66} & C_{26} & 0 \\ C_{26} & C_{22} & 0 \\ 0 & 0 & C_{44} \end{pmatrix}$$

$$\mathbf{c}_{33} = \begin{pmatrix} C_{55} & 0 & 0 \\ 0 & C_{44} & 0 \\ 0 & 0 & C_{33} \end{pmatrix} \quad \mathbf{c}_{23} = \begin{pmatrix} 0 & 0 & C_{36} \\ 0 & 0 & C_{23} \\ 0 & C_{44} & 0 \end{pmatrix}$$

$$\mathbf{c}_{31} = \begin{pmatrix} 0 & 0 & C_{55} \\ 0 & 0 & 0 \\ C_{13} & C_{36} & 0 \end{pmatrix} \quad \mathbf{c}_{12} = \begin{pmatrix} C_{16} & C_{12} & 0 \\ C_{66} & C_{26} & 0 \\ 0 & 0 & 0 \end{pmatrix}.$$

The matrix $\mathbf{A}$ is constructed from these parameter matrices, and if it is divided into four 3×3 sub-matrices $\mathbf{A}_{\mu\nu}$

$$\mathbf{A} = \begin{pmatrix} \mathbf{A}_{11} & \mathbf{A}_{12} \\ \mathbf{A}_{21} & \mathbf{A}_{22} \end{pmatrix}$$

we obtain (6.3.15), (6.3.16) and (6.3.17)

$$\begin{aligned} \mathbf{A}_{22} &= \mathbf{A}_{11}^{\mathrm{T}} = -p_\eta \mathbf{c}_{\eta 3} \mathbf{c}_{33}^{-1} \\ \mathbf{A}_{12} &= -\mathbf{c}_{33}^{-1} \\ \mathbf{A}_{21} &= p_\eta p_\nu \mathbf{c}_{\eta\nu} - \rho \mathbf{I} - p_\eta p_\nu \mathbf{c}_{\eta 3} \mathbf{c}_{33}^{-1} \mathbf{c}_{3\nu}, \end{aligned} \tag{6.8.9}$$

with summations over indices 1 and 2. Thus in monoclinic media we have

$$\begin{aligned} \mathbf{A}_{12} &= -\begin{pmatrix} 1/C_{55} & 0 & 0 \\ 0 & 1/C_{44} & 0 \\ 0 & 0 & 1/C_{33} \end{pmatrix} \\ \mathbf{A}_{22} &= \mathbf{A}_{11}^{\mathrm{T}} = -\begin{pmatrix} 0 & 0 & (p_1 C_{13} + p_2 C_{36})/C_{33} \\ 0 & 0 & (p_1 C_{36} + p_2 C_{23})/C_{33} \\ p_1 & p_2 & 0 \end{pmatrix}. \end{aligned}$$

Matrix $\mathbf{A}_{21}$ has many more terms but is constructed from matrices $\mathbf{I}$, $\mathbf{c}_{11}$, $\mathbf{c}_{22}$, $\mathbf{c}_{12}$ and

$$\begin{aligned} \mathbf{c}_{13}\mathbf{c}_{33}^{-1}\mathbf{c}_{31} &= \begin{pmatrix} C_{13}^2/C_{33} & C_{13}C_{36}/C_{33} & 0 \\ C_{13}C_{36}/C_{33} & C_{36}^2/C_{33} & 0 \\ 0 & 0 & C_{55} \end{pmatrix} \\ \mathbf{c}_{23}\mathbf{c}_{33}^{-1}\mathbf{c}_{32} &= \begin{pmatrix} C_{36}^2/C_{33} & C_{23}C_{36}/C_{33} & 0 \\ C_{23}C_{36}/C_{33} & C_{23}^2/C_{33} & 0 \\ 0 & 0 & C_{44} \end{pmatrix} \\ \mathbf{c}_{13}\mathbf{c}_{33}^{-1}\mathbf{c}_{32} &= \left(\mathbf{c}_{23}\mathbf{c}_{33}^{-1}\mathbf{c}_{31}\right)^{\mathrm{T}} = \begin{pmatrix} C_{13}C_{36}/C_{33} & C_{13}C_{23}/C_{33} & 0 \\ C_{36}^2/C_{33} & C_{23}C_{36}/C_{33} & 0 \\ 0 & 0 & 0 \end{pmatrix}. \end{aligned}$$

The important thing is that although there are lots of terms, all these matrices and therefore $\mathbf{A}_{21}$ are of the form

$$\mathbf{A}_{21} = \begin{pmatrix} \times & \times & 0 \\ \times & \times & 0 \\ 0 & 0 & \times \end{pmatrix},$$

where the cross indicates a non-zero element. Overall the matrix $\mathbf{A}$ has the form

$$\mathbf{A} = \begin{pmatrix} 0 & 0 & \times & \times & 0 & 0 \\ 0 & 0 & \times & 0 & \times & 0 \\ \times & \times & 0 & 0 & 0 & \times \\ \times & \times & 0 & 0 & 0 & \times \\ \times & \times & 0 & 0 & 0 & \times \\ 0 & 0 & \times & \times & \times & 0 \end{pmatrix}.$$

Noting where the zero elements are, we interchange the third and sixth rows and columns in the eigen-system, corresponding to v_3 and σ_{33}, which can be achieved by pre- and post-multiplying by the matrix

$$\mathbf{I}_{36} = \begin{pmatrix} 1 & 0 & 0 & 0 & 0 & 0 \\ 0 & 1 & 0 & 0 & 0 & 0 \\ 0 & 0 & 0 & 0 & 0 & 1 \\ 0 & 0 & 0 & 1 & 0 & 0 \\ 0 & 0 & 0 & 0 & 1 & 0 \\ 0 & 0 & 1 & 0 & 0 & 0 \end{pmatrix},$$

and obtain a modified eigen-system

$$\mathbf{A}'\mathbf{w}' = p_n\mathbf{w}',$$

where

$$\mathbf{A}' = \mathbf{I}_{36}\mathbf{A}\mathbf{I}_{36} = \begin{pmatrix} \mathbf{0} & \mathbf{A}'_{12} \\ \mathbf{A}'_{21} & \mathbf{0} \end{pmatrix},$$

with the diagonal 3×3 blocks zero, and

$$\mathbf{w}' = \mathbf{I}_{36}\mathbf{w} = \begin{pmatrix} v_1 \\ v_2 \\ \sigma_{33} \\ \sigma_{13} \\ \sigma_{23} \\ v_3 \end{pmatrix} = \begin{pmatrix} \mathbf{w}'_1 \\ \mathbf{w}'_2 \end{pmatrix}, \text{ say.}$$

The sub-matrices are

$$\begin{aligned} \mathbf{A}'_{12} &= \begin{pmatrix} A_{14} & A_{15} & A_{13} \\ A_{24} & A_{25} & A_{23} \\ A_{64} & A_{65} & A_{63} \end{pmatrix} \\ \mathbf{A}'_{21} &= \begin{pmatrix} A_{41} & A_{42} & A_{46} \\ A_{51} & A_{52} & A_{56} \\ A_{31} & A_{32} & A_{36} \end{pmatrix}. \end{aligned}$$

The eigen-system can be expanded as

$$\begin{aligned} \mathbf{A}'_{12}\mathbf{w}'_2 &= p_n\mathbf{w}'_1 \\ \mathbf{A}'_{21}\mathbf{w}'_1 &= p_n\mathbf{w}'_2, \end{aligned}$$

and hence

$$\begin{aligned} \left(\mathbf{A}'_{12}\mathbf{A}'_{21}\right)\mathbf{w}'_1 &= p_n^2\mathbf{w}'_1 \\ \left(\mathbf{A}'_{21}\mathbf{A}'_{12}\right)\mathbf{w}'_2 &= p_n^2\mathbf{w}'_2. \end{aligned}$$

These two eigen-systems are equivalent as both $\mathbf{A}'_{12}$ and $\mathbf{A}'_{21}$ are symmetric (as $A_{15} = A_{24} = 0$, $A_{42} = A_{51}$ from elements of matrix $\mathbf{A}_{21}$, and $A_{13} = A_{64}$, $A_{23} = A_{65}$, $A_{46} = A_{31}$ and $A_{56} = A_{32}$ as $\mathbf{A}_{22} = \mathbf{A}_{11}^{\mathrm{T}}$). The matrix $\mathbf{A}'_{12}\mathbf{A}'_{21}$ has right-eigenvector $\mathbf{w}'_1$ and left-eigenvector $\mathbf{w}'_2$; for the matrix $\mathbf{A}'_{12}\mathbf{A}'_{21}$, the roles of the eigenvectors are reversed.

Thus we have reduced the sixth-order eigen-system to a third-order system for the eigenvalues p_n^2. Hence, the original eigenvalues must be in positive and negative pairs. In the eigenvectors, $\mathbf{w}'$, the second part, $\mathbf{w}'_2$, changes sign with p_n. These results agree with the physical requirements in media with up-down symmetry. There is always a sign ambiguity in the definition of eigenvectors. The signs can always be chosen to be consistent with the above rule that $\mathbf{w}'_1$ does not change sign but $\mathbf{w}'_2$ changes sign with p_n. Note that the signs in definitions (6.3.5), (6.3.51), (6.3.52) and (6.3.53) are consistent with this rule.

Isotropic case (2 parameters): The matrix $\mathbf{A}$ in an isotropic medium is given by equation (6.3.47). Thus the sub-matrices are

$$\begin{aligned} \mathbf{A}'_{12} &= -\begin{pmatrix} 1/\mu & 0 & p \\ 0 & 1/\mu & 0 \\ p & 0 & \rho \end{pmatrix} \\ \mathbf{A}'_{21} &= \begin{pmatrix} \eta p^2 - \rho & 0 & -p\lambda/(\lambda+2\mu) \\ 0 & \mu p^2 - \rho & 0 \\ -p\lambda/(\lambda+2\mu) & 0 & -1/(\lambda+2\mu) \end{pmatrix}, \end{aligned}$$

where η is defined in equation (6.3.48). The 3×3 matrix for the eignevalues p_n^2 is

$$\mathbf{A}'_{12}\mathbf{A}'_{21} = \begin{pmatrix} \frac{\rho}{\mu} - \frac{3\lambda+4\mu}{\lambda+2\mu}p^2 & 0 & \frac{\lambda+\mu}{\mu(\lambda+2\mu)}p \\ 0 & \frac{\rho}{\mu} - p^2 & 0 \\ 2p\left(\rho - 2\mu p^2\right)\frac{\lambda+\mu}{\lambda+2\mu} & 0 & \frac{\rho+\lambda p^2}{\lambda+2\mu} \end{pmatrix}.$$

Although the *SH* eigenvalue is obvious, the *P-SV* result is not obvious

but straightforward algebra shows

$$\left|\mathbf{A}'_{12}\mathbf{A}'_{21} - p_n^2\mathbf{I}\right| = \left(\frac{\rho}{\mu} - p^2 - p_n^2\right)^2 \left(\frac{\rho}{\lambda+2\mu} - p^2 - p_n^2\right) = 0,$$

giving the expected eigenvalues.

TIV case (5 parameters): From the matrix $\mathbf{A}$ (6.3.64), the sub-matrices are

$$\begin{aligned}
\mathbf{A}'_{12} &= -\begin{pmatrix} 1/C_{44} & 0 & p \\ 0 & 1/C_{44} & 0 \\ p & 0 & \rho \end{pmatrix} \\
\mathbf{A}'_{21} &= \begin{pmatrix} p^2(C_{11} - C_{13}^2/C_{33}) - \rho & 0 & -p\,C_{13}/C_{33} \\ 0 & p^2\,C_{66} - \rho & 0 \\ -p\,C_{13}/C_{33} & 0 & -1/C_{33} \end{pmatrix}.
\end{aligned}$$

The eigen-matrix is

$$\mathbf{A}'_{12}\mathbf{A}'_{21} = \begin{pmatrix} \frac{\rho}{C_{44}} + p^2\,\frac{C_{13}^2+C_{13}C_{44}-C_{11}C_{33}}{C_{33}C_{44}} & 0 & p\,\frac{C_{13}+C_{44}}{C_{33}C_{44}} \\ 0 & \frac{\rho}{C_{44}} - p^2\,\frac{C_{66}}{C_{44}} & 0 \\ p^3\,\frac{C_{13}^2-C_{11}C_{33}}{C_{33}} + \rho p\,\frac{C_{13}+C_{33}}{C_{33}} & 0 & \frac{\rho}{C_{33}} + p^2\,\frac{C_{13}}{C_{33}} \end{pmatrix}.$$

After some algebra, the eigenvalue equation can be reduced to

$$\left|\mathbf{A}'_{12}\mathbf{A}'_{21} - p_n^2\,\mathbf{I}\right| = \frac{1}{A_{33}A_{44}}\left(\frac{1}{A_{44}} - p^2\,\frac{A_{66}}{A_{44}} - p_n^2\right)\left[A_{33}A_{44}p_n^4 - Bp_n^2 + (A_{11}p^2 - 1)(A_{44}p^2 - 1)\right],$$

where B is defined by equation (5.7.33) with (5.7.31) and (5.7.20), and just here $A_{ij} = C_{ij}/\rho$ are the density-normalized elastic parameters not elements of the matrix $\mathbf{A}$. Clearly the *qSH* root agrees with result (5.7.24), and the *qP*-*qSV* roots from the quadratic for p_n^2 agree with solutions (5.7.32).

monoclinic (12 parameters): We discuss the general monoclinic system next with 12 parameters, as in the simpler orthorhombic medium only 3 more parameters are zero. The general 3×3 matrices of elastic parameters (4.4.39) have been given above. The sub-matrices $\mathbf{A}_{11}$ and $\mathbf{A}_{22}$ (6.3.15) and $\mathbf{A}_{12}$ (6.3.16) of the matrix $\mathbf{A}$ have been given above and the elements of the sub-matrix $\mathbf{A}_{21}$ (6.3.17) are

$$\begin{aligned}
A_{41} &= p_1^2(C_{11} - C_{13}^2/C_{33}) + p_2^2(C_{66} - C_{36}^2/C_{33}) \\
&\quad + 2p_1p_2(C_{16} - C_{13}C_{36}/C_{33}) - \rho
\end{aligned}$$

$$
\begin{aligned}
A_{52} &= p_1^2(C_{66} - C_{36}^2/C_{33}) + p_2^2(C_{22} - C_{23}^2/C_{33}) \\
&\quad + 2p_1p_2(C_{26} - C_{23}C_{36}/C_{33}) - \rho \\
A_{63} &= -\rho \\
A_{51} &= A_{42} = p_1^2(C_{16} - C_{13}C_{36}/C_{33}) + p_2^2(C_{26} - C_{23}C_{36}/C_{33}) \\
&\quad + p_1p_2(C_{12} + C_{66} - C_{13}C_{23}/C_{33} - C_{36}^2/C_{33}) \\
A_{61} &= A_{62} = A_{43} = A_{53} = 0.
\end{aligned}
$$

The matrices of the third-order system are

$$
\mathbf{A}'_{12} = -\begin{pmatrix} 1/C_{55} & 0 & p_1 \\ 0 & 1/C_{44} & p_2 \\ p_1 & p_2 & \rho \end{pmatrix}
$$

$$
\mathbf{A}'_{21} =
$$

$$
\begin{pmatrix} & A_{41} & & A_{51} & & -(p_1C_{13} + p_2C_{36})/C_{33} \\ & A_{51} & & A_{52} & & -(p_1C_{36} + p_2C_{23})/C_{33} \\ -(p_1C_{13} + p_2C_{36})/C_{33} & & -(p_1C_{36} + p_2C_{23})/C_{33} & & -1/\rho & \end{pmatrix},
$$

where the 3 long elements in the upper-left 2×2 have not been repeated. It is easily checked that these results reduce to the isotropic and TIV results.

To find the eigenvalues of the third-order system we need to expand and solve

$$
\left| \mathbf{A}'_{12}\mathbf{A}'_{21} - p_n^2\,\mathbf{I} \right| = 0.
$$

This reduces to a cubic, but having found the matrices $\mathbf{A}'_{12}$ and $\mathbf{A}'_{21}$ algebraically there is little point in proceeding further as the algebra does not simplify. It is straightforward to find the coefficients of the cubic numerically. An analytic solution is available for a cubic. Although this used to be textbook stuff, it is perhaps less well known now. The procedure is:

consider the cubic in its standard form

$$
x^3 + px^2 + qx + r = 0.
$$

This can be reduced to

$$
y^3 + 3Qy - 2R = 0,
$$

where

$$
\begin{aligned}
y &= x + \frac{p}{3} \\
3Q &= q - \frac{1}{3}p^2
\end{aligned}
$$

$$2R = \frac{p}{3}\left(q - \frac{2p^2}{9}\right) - r.$$

We define a discriminant

$$D = Q^3 + R^2.$$

If $D > 0$, there is one real root, and if $D \leq 0$ there are three real roots (multiple roots if $D = 0$). The following algorithms require the special case of a triple root when $Q = R = 0$, and $y_1 = y_2 = y_3 = 0$, to be handled separately.

If $D > 0$ we make the transformation

$$y = 2Q^{1/2} \sinh \frac{\theta}{3},$$

and the cubic reduces to

$$\sinh \theta = \frac{R}{Q^{3/2}}.$$

The standard logarithmic formula for the inverse hyperbolic sine gives

$$\frac{\theta}{3} = \ln \frac{S}{Q^{1/2}},$$

where

$$S = \left(R + \sqrt{D}\right)^{1/3}.$$

Substituting, this gives the root

$$y_1 = S + T,$$

where

$$T = -Q/S = \left(R - \sqrt{D}\right)^{1/3}.$$

If $R < 0$ it is best to calculate T first and derive S from it.

If $D < 0$, then we make the transformation

$$y = 2(-Q)^{1/2} \cos \frac{\theta}{3},$$

and the cubic reduces to

$$\cos \theta = \frac{R}{(-Q)^{3/2}}$$

(necessarily $Q < 0$). The solutions are

$$\begin{aligned} y_1 &= 2\sqrt{-Q}\cos\frac{\theta}{3} \\ y_1 &= 2\sqrt{-Q}\cos\left(\frac{\theta}{3}+\frac{2\pi}{3}\right) \\ y_1 &= 2\sqrt{-Q}\cos\left(\frac{\theta}{3}+\frac{4\pi}{3}\right). \end{aligned}$$

orthorhombic case (9 parameters): An orthorhombic medium is characterized by a stiffness Voigt matrix

$$\mathbf{C} = \begin{pmatrix} C_{11} & C_{12} & C_{13} & 0 & 0 & 0 \\ C_{12} & C_{22} & C_{23} & 0 & 0 & 0 \\ C_{13} & C_{23} & C_{33} & 0 & 0 & 0 \\ 0 & 0 & 0 & C_{44} & 0 & 0 \\ 0 & 0 & 0 & 0 & C_{55} & 0 \\ 0 & 0 & 0 & 0 & 0 & C_{66} \end{pmatrix}$$

(Schoenberg and Helbig, 1997†, and references therein). This results in some simplification of the monoclinic results above, but in general it is probably best to proceed numerically from the matrices $\mathbf{A}'_{12}$ and $\mathbf{A}'_{21}$ to the solution of the cubic. Only if $p_1 = 0$ or $p_2 = 0$, i.e. on a plane of symmetry, do the results simplify significantly. Then the form simplifies to that in TIV media, and the solution reduces to a simple equation for the qS wave transverse to the symmetry plane, and a quadratic equation for the qP-qS waves in the symmetry plane.

- *Page 250:* **Erratum** — the text and equations on page 250 are confused. Apart from sign errors, differential equations for $\mathbf{v}$ and $\mathbf{w}$ have got mixed up. The page should read:

  Transforming, the equation of motion (4.5.1) becomes

$$-\mathrm{i}\,\omega\rho(z)\mathbf{v} = -\begin{pmatrix} \mathrm{i}\,\omega p \\ \partial/\partial z \end{pmatrix} P - A_{\mathsf{S}} P_{\mathsf{S}}(\omega) \begin{pmatrix} \mathrm{i}\,\omega p\,\delta(z-z_{\mathsf{S}}) \\ \delta'(z-z_{\mathsf{S}}) \end{pmatrix}, \quad (7.1.13)$$

  cf. equation (7.1.1). Equivalent to equation (7.1.4), we have

$$\frac{\mathrm{d}}{\mathrm{d}z}\mathbf{w} = \mathrm{i}\,\omega\mathbf{A}\,\mathbf{w} - A_{\mathsf{S}} P_{\mathsf{S}}(\omega) \begin{pmatrix} \mathrm{i}\,\omega p^2\,\delta(z-z_{\mathsf{S}})/\rho \\ -\delta'(z-z_{\mathsf{S}}) \end{pmatrix}. \quad (7.1.14)$$

  If the source is in a homogeneous region and anticipating the fundamental

† Schoenberg, M. and Helbig, K., 1997. Orthorhombic media: modelling elastic wave behavior in a vertically fractured earth, *Geophysics*, **62**, 1954–74.

solution (7.2.2) (so $\delta'(z - z_S) \to \pm \mathrm{i}\,\omega q_\alpha \delta(z - z_S)$ for the plane-wave solutions propagating in the positive and negative directions), the response for a pressure line source can be obtained from the Green function by post-multiplying the solution by a 'force' factor

$$\mathbf{f} = -\mathrm{i}\,\omega A_S P_S(\omega) \begin{pmatrix} p \\ \pm q_\alpha \end{pmatrix}, \tag{7.1.15}$$

i.e. the combination $\boldsymbol{\mathcal{F}}\,\mathbf{f}\,\delta(z - z_S)$ in equation (7.1.4) is equivalent to the source term in equation (7.1.14) (as expected, a 'force' in the direction of the wave normal). In the time domain, the Green function is convolved with $A_S P'_S(t)$ and the pressure source is represented by the 'force' factor

$$\mathbf{f} = \begin{pmatrix} p \\ \pm q_\alpha \end{pmatrix} A_S P'_S(t) * = -\begin{pmatrix} p \\ \pm q_\alpha \end{pmatrix} M_S, \tag{7.1.16}$$

where the final expression corresponds to the moment tensor source (4.6.7) with (4.6.21).

The sign errors do not persist on later pages.

- *Page 285, equation (7.2.129)* **Addendum** — in equation (7.2.129), the sign of the increments is ambiguous. The sentence is better rewritten: For from equation (6.3.7) (with the increments taken in the positive z direction)

$$\mathcal{T}_{11} = -\mathcal{T}_{22} = \frac{\rho_2 q_{\alpha\,1} - \rho_1 q_{\alpha\,2}}{\rho_2 q_{\alpha\,1} + \rho_1 q_{\alpha\,2}} \simeq \frac{\delta(q_\alpha/\rho)}{2q_\alpha/\rho} \simeq \gamma_A\ \delta\zeta. \tag{7.2.129}$$

- *Page 292:* **Erratum** — in equation (7.2.164), the rows of matrix $\mathbf{L}$ are interchanged. It should read

$$\mathbf{L} = (\mu p)^{-1/2} \begin{pmatrix} 0 & 1 \\ \mu p & 0 \end{pmatrix}. \tag{7.2.164}$$

As a consequence, equation (7.2.165) has a sign error and should be

$$\frac{\mathrm{d}\mathbf{y}}{\mathrm{d}z} = \mathrm{i}\,\omega\,\mathbf{B}\,\mathbf{y} + \frac{\mu'}{2\mu}\,\mathbf{I}_3. \tag{7.2.165}$$

- *Page 297:* **Erratum** — between equations (7.2.190) and (7.2.191), the order of the expressions is reversed. It should read " $\ldots (2p/q_\beta)^{1/2}$ and $(2p/q_\alpha)^{1/2}$, respectively, $\ldots$".

- *Pages 299 to 308:* **Revision** — the algorithm is revised to use the travelling rather than standing-wave solution. This improves the numerical behaviour and avoids overflow. The text has been revised to reflect this and simplified by omitting some details. On page 209, following equation (7.2.202), the revised text reads

  with $d = z_{\mathrm{A}} - z_{\mathrm{B}}$, the layer thickness. $\mathbf{X}_V$ and $\mathbf{X}_P$ are defined with the appropriate vertical slowness, q_V or q_P, and g_V or g_P, respectively. For numerical purposes, it is better to factor the propagator using the travelling wave solutions as in evanescent regions these remain independent. The eigenvalues of the matrix (7.2.176) are $\pm q_\nu$, and the eigenvectors can be written as a 2×2 matrix

$$\mathbf{Y}_\nu = 2^{-1/2} \begin{pmatrix} 1/h_\nu & -1/h_\nu \\ -h_\nu & -h_\nu \end{pmatrix}, \tag{7.2.203}$$

  i.e. $\mathbf{B}_\nu \mathbf{Y}_\nu = \mathbf{Y}_\nu \mathbf{p}_\nu$, cf. equation (6.3.3), where for convenience we have defined $h_\nu^2 = -g_\nu$. It is then easily shown that for (7.2.198)

$$\mathbf{L}(\mathbf{Y}_V \oplus \mathbf{Y}_P) = \mathbf{W} \begin{pmatrix} 1 & 0 & 0 & 0 \\ 0 & 0 & 1 & 0 \\ 0 & -1 & 0 & 0 \\ 0 & 0 & 0 & 1 \end{pmatrix} = \mathbf{W}\mathbf{I}^{\S} = \mathbf{W}^{\S}, \tag{7.2.204}$$

  say, where $\mathbf{W}$ is defined in equations (6.3.51) and (6.3.53), reduced to the 4×4 P – SV system. The interchange of the second and third columns of $\mathbf{W}$ in $\mathbf{W}^{\S}$ is necessary to group the SV and P solutions and obtain the block diagonal form $\mathbf{Y} = \mathbf{Y}_V \oplus \mathbf{Y}_P$. The sign change of the third column of $\mathbf{W}$, the SV solution propagating in the negative direction, is necessary to obtain the sign change in the elements of $\mathbf{W}^{\S}$ containing q_V (in (6.3.51), the other elements change sign in order to emphasize the up/down symmetry, see Exercise 6.4). Similar but simpler expressions to (7.2.204) hold for acoustic waves ((6.3.5) and (7.2.132)) and SH waves ((6.3.52) and (7.2.164)).

  With the factorization (7.2.204), the Haskell matrix (7.2.4) (the propagator in a homogeneous layer) can be written

$$\mathbf{P}(z, z_0) = \mathbf{L}\,\mathbf{Y} \mathrm{e}^{\mathrm{i}\,\omega \mathbf{p}_z^{\S}(z - z_0)} \mathbf{Y}^{-1} \mathbf{L}^{-1}, \tag{7.2.205}$$

  where

$$\mathbf{Y} = \mathbf{Y}_V \oplus \mathbf{Y}_P = (\mathbf{Y}_V \oplus \mathbf{I})(\mathbf{I} \oplus \mathbf{Y}_P), \tag{7.2.206}$$

the inverse matrices are simply

$$\mathbf{Y}_\nu^{-1} = 2^{-1/2} \begin{pmatrix} h_\nu & -1/h_\nu \\ -h_\nu & -1/h_\nu \end{pmatrix}, \tag{7.2.207}$$

and the transformation matrix in equation (7.2.204), $\mathbf{I}^{\S}$, simply alters the order of the eignevalues in the diagonal matrix, i.e.

$$\mathbf{p}_z^{\S} = \mathbf{p}_V \oplus \mathbf{p}_P = \begin{pmatrix} q_V & 0 & 0 & 0 \\ 0 & -q_V & 0 & 0 \\ 0 & 0 & q_P & 0 \\ 0 & 0 & 0 & -q_P \end{pmatrix}, \tag{7.2.208}$$

compared with (7.2.4). Similar but simpler expressions apply for the acoustic and *SH* Haskell matrices.

Pages 300 to 303 are unaltered except that the equation numbers are increased by 4. Pages 304 to 308 are revised to

Result (7.2.220) applies however the propagator is obtained. With the Langer decomposition (7.2.205) , it is particularly simple as the matrices (7.2.187), (7.2.188) and (7.2.206) have been factorized, and the individual matrices contain many zero, unit or equal elements. Thus the main term from the stack of layers is

$$\begin{aligned} \mathbf{Z} \;=\; & \{\, \mathrm{e}^{\mathrm{i}\,\omega \mathbf{p}_1^{\S} d_1} \,\} \{\mathbf{Y}_1^{-1}\} \{\mathbf{L}_1^{-1}\} \\ & \times \left(\prod_{j=2}^{n-1} \{\mathbf{L}_j\} \{\mathbf{Y}_j\} \{\, \mathrm{e}^{\mathrm{i}\,\omega \mathbf{p}_j^{\S} d_j} \,\} \{\mathbf{Y}_j^{-1}\} \{\mathbf{L}_j^{-1}\} \right) \{\mathbf{L}_n\} \{\mathbf{Y}_n\}, \end{aligned} \tag{7.2.221}$$

where

$$\{\overline{\mathbf{P}}\} = \{\mathbf{W}_1^{-1} \mathbf{L}_1 \mathbf{Y}_1\} \mathbf{Z} \{\mathbf{Y}_n^{-1} \mathbf{L}_n^{-1} \mathbf{W}_n\}. \tag{7.2.222}$$

As

$$\{\mathbf{W}^{-1}\mathbf{L}\mathbf{Y}\} = \{\mathbf{I}^{\S}\} = \begin{pmatrix} 0 & 1 & 0 & 0 & 0 & 0 \\ -1 & 0 & 0 & 0 & 0 & 0 \\ 0 & 0 & 1 & 0 & 0 & 0 \\ 0 & 0 & 0 & 1 & 0 & 0 \\ 0 & 0 & 0 & 0 & 0 & 1 \\ 0 & 0 & 0 & 0 & -1 & 0 \end{pmatrix}, \tag{7.2.223}$$

from equation (7.2.204), equation (7.2.220) can be rewritten as

$$\mathbf{R}_{n\,2} = -\frac{1}{Z_{55}}\begin{pmatrix} Z_{35} & Z_{15} \\ Z_{65} & -Z_{45} \end{pmatrix}. \tag{7.2.224}$$

Even for a single interface ($n = 2$), this reduces to a simple algorithm for the interface coefficients with

$$\mathbf{Z} = \{\mathbf{Y}_1^{-1}\}\,\{\mathbf{L}_1^{-1}\}\{\mathbf{L}_2\}\,\{\mathbf{Y}_2\}\,. \tag{7.2.225}$$

With expression (7.2.225) substituted in result (7.2.224) we obtain results equal to the standard interface coefficients (e.g. equations (6.3.60)–(6.3.62) for the isotropic coefficients) but with a relatively simple algorithm.

With the Langer block-diagonal decomposition (7.2.201) and factorization (7.2.187), (7.2.188) and (7.2.206), the second-order minors are particularly simple to compute. Ignoring the trailing diagonal matrix in expression (7.2.187), which simply forms a diagonal matrix of second-order minors and reduces to a simple scaling, we have

$$\{\mathbf{L}\} \doteq \begin{pmatrix} 1 & 0 & 0 & 0 & 1 & 0 \\ -Z_P & 0 & 0 & 0 & -Z_V & 0 \\ 0 & 0 & 0 & -1 & 0 & 0 \\ 0 & 0 & Z_V - Z_P & 0 & 0 & 0 \\ 0 & 1 & 0 & 0 & 0 & 1 \\ 0 & -Z_P & 0 & 0 & 0 & -Z_V \end{pmatrix} \times \begin{pmatrix} 1 & 0 & 0 & 0 & 1 & 0 \\ -Z_V & 0 & 0 & 0 & -Z_P & 0 \\ 0 & 0 & 0 & -1 & 0 & 0 \\ 0 & 0 & Z_P - Z_V & 0 & 0 & 0 \\ 0 & 1 & 0 & 0 & 0 & 1 \\ 0 & -Z_V & 0 & 0 & 0 & -Z_P \end{pmatrix} \tag{7.2.226}$$

(where the symbol $\doteq$ is used to indicate that the unimportant, diagonal matrix is missing). Multiplication by the matrix $\{\mathbf{L}\}$ can be performed by the repeated applications of the sub-matrix

$$\begin{pmatrix} 1 & 1 \\ -Z_P & -Z_V \end{pmatrix}, \tag{7.2.227}$$

with the appropriate row and column indices. A similar, simple expression is obtaining for the inverse matrix from expression (7.2.188), again ignoring the leading diagonal matrix.

For the matrices $\mathbf{Y}$, we can ignore the factors $2^{-1/2}$ as they simply scale the solution, and with the factorization (7.2.206) the second-order minor expression is

$$\{\mathbf{Y}_V \oplus \mathbf{I}\} \doteq \begin{pmatrix} -2 & 0 & 0 & 0 & 0 & 0 \\ 0 & 1/h_\nu & 0 & -1/h_\nu & 0 & 0 \\ 0 & 0 & 1/h_\nu & 0 & -1/h_\nu & 0 \\ 0 & -h_\nu & 0 & -h_\nu & 0 & 0 \\ 0 & 0 & -h_\nu & 0 & -h_\nu & 0 \\ 0 & 0 & 0 & 0 & 0 & 1 \end{pmatrix}, \tag{7.2.228}$$

and similarly for $\{\mathbf{I} \oplus \mathbf{Y}_P\}$.

For the phase term we obtain

$$\{\mathrm{e}^{\mathrm{i}\,\omega \mathbf{p}_z^{\S}}\} = \begin{pmatrix} 1 & 0 & 0 & 0 & 0 & 0 \\ 0 & e_V e_P & 0 & 0 & 0 & 0 \\ 0 & 0 & e_V/e_P & 0 & 0 & 0 \\ 0 & 0 & 0 & e_P/e_V & 0 & 0 \\ 0 & 0 & 0 & 0 & 1/e_V e_P & 0 \\ 0 & 0 & 0 & 0 & 0 & 1 \end{pmatrix}, \tag{7.2.229}$$

where $e_\nu = \exp(\mathrm{i}\,\omega q_\nu d)$, although computationally we replace the matrix (7.2.229) by $e_V e_P \{\mathrm{e}^{\mathrm{i}\,\omega \mathbf{p}_z^{\S}}\}$ to avoid overflow.

The algorithm is so straightforward that a Matlab program has been included in Chapman (2003) for the isotropic case, although that contained a sign error (Chapman, 2005) and used the standing-wave solution (7.2.201) so numerical overflow could occur. Multiplications of the six-dimensional vector by the matrices of second-order minors in (7.2.221) is performed using the factorizations (7.2.226) for $\mathbf{L}$, and (7.2.228) for $\mathbf{Y}$, and similarly for the inverses, etc. Clearly because of their repetitive nature, these operations will be extremely simple and efficient to code and compute. A complete algorithm would need to handle some special cases: $p = 0$, $\mu = 0$ or $q = 0$. The method is best described as the *factorized Haskell (second-order minor) matrix method.*

The revised version of the routine `Rcoefficients`, given in Exercise 7.6 is

```
function [ Rvv, Rpv, Rvp, Rpp ] = ...
  Rcoefficients( mat, p, omegas, properties )
% Rcoefficients - P-SV reflection coefficients from layer
%                 stack using algorithm in Section 7.2.8

% INPUT:
%         mat                 = 'Iso' use Iso_PSV_EigenFactors
```

```
%                               = 'TIV' use TIV_PSV_EigenFactors
%         p                     = horizontal slowness
%         omegas                = circular frequencies
%
%         if mat = 'Iso':
%         properties(i).Alpha = P velocities
%         properties(i).Beta  = S velocities
%
%         if mat = 'TIV':
%         properties(i).C11   = C11 stiffness
%         properties(i).C33   = C33 stiffness
%         properties(i).C44   = C44 stiffness
%         properties(i).C13   = C13 stiffness
%
%         properties(i).Rho   = densities
%         properties(i).Thick = layer thickness
%
%           coefficients are properties(1).Thick above
%           interface and properties(nLayers).Thick is
%           ignored
%
%           stiffnesses may be frequency arrays for attenuation which
%           should match omegas arrray.  They must be row vectors
%           e.g. 1 x nOmega.
%
% OUTPUT:
%         Rvv           = VV coeficient
%         Rpv           = PV coeficient (P incident)
%         Rvp           = VP coeficient (SV incident)
%         Rpp           = PP coeficient
%
% NOTE:
%
% properties(*).Alpha etc. must be scalars or nOmega arrays to
% include frequency-dependent velocities to model attenuation
% (the attenuation model is therefore created externally);
% in this simplified version -
% p=0, Beta=0, p*Alpha=1 or p*Beta=1 are not allowed;
% code is so simply we don't use functions except for
% 'mat'_PSV_EigenFactors and LayerPhase;
% the code is written to allow for frequency arrays of velocity
% or not;
%
% As revised for Addenda and Errata, 25 November 2004
% Revised numerical normalization rather than analytic
% factor, 18 Dec 2005
% Revised to use travelling solutions, with revised
% arguments, 22 January 2007
%
nLayers = length(properties);
```

```
nOmega  = length(omegas);
%
% loop from bottom to top
for j = nLayers:-1:1
  %
  % eigenfactors of j-th layer
  eval([ '[qV,qP,ZV,ZP,gV,gP,sV,sP] = ' ...
        mat 'PSVEigenFactors(p,properties(j));' ]);
  %
  % starting condition in lower half space,
  % sixth column of Y^-1 L^-1 W - equation (7.2.223)
  if j == nLayers
    % force correct frequency array size
    x1 = zeros(1,nOmega);
    x2 = x1;
    x3 = x1;
    x4 = x1;
    x5 = ones(1,nOmega);
    x6 = x1;
  %
  % propagate through j-th layer
  else
    %
    % multiply by L^-1
    % temporary vector is (wa,wb,.,.,wc,wd)
    % first matrix multiply
    wa = ZV.*x1+x2;
    wb = ZV.*x5+x6;
    wc = -ZP.*x1-x2;
    wd = -ZP.*x5-x6;
    % second matrix multiply
    x1 = -ZP.*wa-wb;
    x2 = -ZP.*wc-wd;
    x5 = ZV.*wa+wb;
    x6 = ZV.*wc+wd;
    % scale (minus sign in theory is not strictly necessary
    % as it cancels with previous scaling in L for (j+1))
    dZ = ZV-ZP;
    x3 =  dZ.*x3;
    x4 = -dZ.*x4;
    %
    % multiply by Y^-1
    % temporary vector is (.,wa,wb,wc,wd,.)
    wa = x2+x3./gP;
    wb = x3-x2.*gP;
    wc = x4+x5./gP;
    wd = x5-x4.*gP;
    %
    x2 = wa+wc./gV;
    x3 = wb+wd./gV;
```

```
    x4 = wc-wa.*gV;
    x5 = wd-wb.*gV;
    %
    x1 = 2*x1; x6 = 2*x6;
    %
    % multiply by exp(i omega q d) (avoid if only DC)
    % equation (7.2.229)
    if ( nOmega > 1 || omegas(1) ~= 0 )
      thick = properties(j).Thick;
      % P and SV phases
      PposExp = LayerPhase(omegas,thick,qP);
      VposExp = LayerPhase(omegas,thick,qV);
      wa = PposExp.*VposExp;
      % include phase with 1/(PposExp*VposExp) removed to
      % avoid overflow
      x1 = wa.*x1;
      x2 = wa.*wa.*x2;
      x3 = VposExp.*VposExp.*x3;
      x4 = PposExp.*PposExp.*x4;
      x6 = wa.*x6;
    end
  end
  %
  % end condition in first layer
  if j == 1
    %
    % form coefficients
    dZ = sqrt(gV.*gP);
    Rvv = -gV.*x3./x5;
    Rpv =  dZ.*x1./x5;
    Rvp =  dZ.*x6./x5;
    Rpp =  gP.*x4./x5;
  %
  % recombine in j-th layer
  else
    % multiply by Y - equation (7.2.228)
    % temporary vector is (.,wa,wb,wc,wd,.)
    wa = x2-x3./gP;
    wb = x3+x2.*gP;
    wc = x4-x5./gP;
    wd = x5+x4.*gP;
    %
    x2 = wa-wc./gV;
    x3 = wb-wd./gV;
    x4 = wc+wa.*gV;
    x5 = wd+wb.*gV;
    %
    x1 = 2*x1; x6 = 2*x6;
    %
    % multiply by L - equation (7.2.226)
```

```
    % temporary vector is (wa,wb,.,.,wc,wd)
    % first matrix multiply
    wa = x1+x5;
    wb = -ZV.*x1-ZP.*x5;
    wc = x2+x6;
    wd = -ZV.*x2-ZP.*x6;
    % second matrix multiply
    x1 = wc+wa;
    x2 = -ZV.*wc-ZP.*wa;
    x5 = wd+wb;
    x6 = -ZV.*wd-ZP.*wb;
    % scale
    dZ = ZV-ZP;
    x3 =  dZ.*x3;
    x4 = -dZ.*x4;
    %
    % Normalize solution independently at each frequency.
    % Various factors are ommitted, and ZP and ZV may be
    % large or small depending on p and units.
    % Safest solution is to normalize numerically - sqrt
    % postponed for efficiency.
    wt =         max( real(x1).^2+imag(x1).^2, ...
                      real(x2).^2+imag(x2).^2 );
    wt =         max( real(x3).^2+imag(x3).^2, wt );
    wt =         max( real(x4).^2+imag(x4).^2, wt );
    wt =         max( real(x5).^2+imag(x5).^2, wt );
    wt = 1./sqrt(max( real(x6).^2+imag(x6).^2, wt ));
    x1 = x1.*wt; x2 = x2.*wt; x3 = x3.*wt;
    x4 = x4.*wt; x5 = x5.*wt; x6 = x6.*wt;
  end
end
return
```

with revised routines

```
function [ qV, qP, ZV, ZP, gV, gP, sV, sP ] = ...
  IsoPSVEigenFactors( p, properties )
% return eigen-factors for P and SV waves for isotropic medium

% For internal use in algorithm in Section 7.2.8
% For inelastic, vp and vs may be frequency arrays (for attenuation)
% and then q*, Z* and g* will be arrays (s* is scalar).
% For elastic, all are scalars.
% In calling program assumed that arrays match frequencies.
%
ro = properties.Rho;
vp = properties.Alpha;
vs = properties.Beta;
% vertical slownesses - equations (6.2.8) and (6.2.9)
qV = sqrt((1./vs-p).*(1./vs+p));
```

```
qP = sqrt((1./vp-p).*(1./vp+p));
% cross-impedances - equations (7.2.193) and (7.2.194)
ZV = 2*ro*p*(vs.*vs);
ZP = ZV-ro/p;
% polarization (co)tangents - equations (7.2.191)
% and (7.2.192)
gV = -p./qV;
gP = -p./qP;
% scaling factors - equations (7.2.195)
sV = sqrt(p/ro);
sP = sV;
return


function [ qV, qP, ZV, ZP, gV, gP, sV, sP ] = ...
  TIVPSVEigenFactors( p, properties )
% return eigen-factors for P and SV waves for TIV medium

% For internal use in algorithm in Section 7.2.8
% Stiffnesses are either scalars or frequency arrays (for
% attenuation).
% Assumption that all are same size so all internal
% variables will  be same size.
%
A11 = properties.C11/properties.Rho;
A33 = properties.C33/properties.Rho;
A44 = properties.C44/properties.Rho;
A13 = properties.C13/properties.Rho;
%
ps = p*p;
% terms (5.7.20), (5.7.31) and (5.7.33)
aa = A13+A44;
AA = A11.*A33+A44.*A44-aa.*aa;
BB = A33+A44-ps*AA;
% equation (5.7.32) for the normal component of slowness
A34 =2*A33.*A44;
tmp = sqrt(BB.*BB-2*A34.*(A11*ps-1).*(A44*ps-1));
qVs = (BB+tmp)./A34;
qV = sqrt(qVs);
qPs = (BB-tmp)./A34;
qP = sqrt(qPs);
% qSV polarizations (5.7.35)
g1 = 2*p*aa.*qV;
tmp = (A33-A44).*qVs-ps*(A11-A44);
g3 = tmp-sqrt(tmp.*tmp+g1.*g1);
% normal component of group velocity (5.7.37)
V3 = qV.*(ps*AA+A34.*qVs-A33-A44)./ ...
     (ps*(A11+A44)+(A33+A44).*qVs-2);
% energy normalize polarizations
gg = sqrt(g1.*g1+g3.*g3).*sqrt(2*properties.Rho*V3);
g1 = g1./gg;
```

```
g3 = g3./gg;
% traction components (6.3.66)
t31 = -(p*g3+qV.*g1).*properties.C44;
t33 = -p*g1.*properties.C13-qV.*g3.*properties.C33;
%
ZV = t33./g1;
gV = g3./g1;
sV = sqrt(-2*g1.*g3);
% repeat for qP
g1 = 2*p*aa.*qP;
tmp = (A33-A44).*qPs-ps*(A11-A44);
g3 = tmp+sqrt(tmp.*tmp+g1.*g1);
V3 = qP.*(ps*AA+A34.*qPs-A33-A44)./ ...
     (ps*(A11+A44)+(A33+A44).*qPs-2);
gg = sqrt(g1.*g1+g3.*g3).*sqrt(2*properties.Rho*V3);
g1 = g1./gg;
g3 = g3./gg;
t31 = -(p*g3+qP.*g1).*properties.C44;
t33 = -p*g1.*properties.C13-qP.*g3.*properties.C33;
ZP = t33./g1;
gP = -g1./g3;
sP = sqrt(2*g1.*g3);
return


function posExp = LayerPhase( omegas, thick, q )
% return exponential phase term

% For internal use in algorithm in Section 7.2.8 for
% terms in matrix exp(i omega q d) (as in equation (7.2.202)).
%
% NOTE:
% valid for q as frequency array and omegas uneven, but
% tries to use recursive formula.
%
% Im(q) > 0 so this may be exponentially small causing underflow
% and zero (but not overflow and Inf or NaN).
%
nOmega = length(omegas);
iq = i*q;
% if q is array, assumed to be frequency array so
% recursion cannot be used
if length(q) > 0
   posExp = exp(thick*omegas.*iq);
else
% q scalar so try to use recursion formula
   posExp(1) = exp(thick*omegas(1)*iq);
  if ( nOmega > 1 )
    for n = 2:1:nOmega
      % compute delPosExp
      % avoids recomputing for uniform distribution
```

```
        if n == 2
          delO2 = omegas(2)-omegas(1);
          delPosExp = exp(thick*delO2*iq);
        else
          delO1 = delO2;
          delO2 = omegas(n)-omegas(n-1);
          % assumes omegas monotonically increasing
          % frequency increment NOT constant
          if abs(delO1-delO2) > 1.e-6*(delO1+delO2)
              delPosExp = exp(thick*delO2*iq);
          end
        end
        %
         posExp(n) =  posExp(n-1)*delPosExp;
      end
    end
  end
  return
```

- *Page 309:* **Revision** — in Exercise 7.6, add " . . . Chapman, 2003, which should be revised according to Chapman, 2005, and the revised algorithm given in the text)."

- *Page 309:* **Erratum** — in Exercise 7.8, "Investigate the symplectic symmetry proportion . . . " should read "Investigate the symplectic symmetry properties . . . ".

- *Page 309:* **Revision** — in Exercise 7.8, ". . . propagator . . . " should read ". . . propagator matrix . . . ".

- *Page 353:* **Addendum** — on the second line of page 353 in Chapter 8, the forward reference to Section 9.1.3 could usefully also refer to Section 9.2.6 .

- *Page 376, Exercise 8.5 and Solutions page 135:* **Appendum** — Exercise 8.5 could have contained interesting *Further reading*.

  Further reading: a related problem is the dispersion of gravity water waves or tsunamis. Jeffreys and Jeffreys (1962, Section 17.09) † have given the basic theory which gives rise to another Airy Phase (see Exercise 8.4).

  This material for *Further reading* was written on 31 December 2004 on

† Jeffreys, H. and Jeffreys, B.S. 1962. *Methods of Mathematical Physics*, Cambridge: Cambridge University Press.

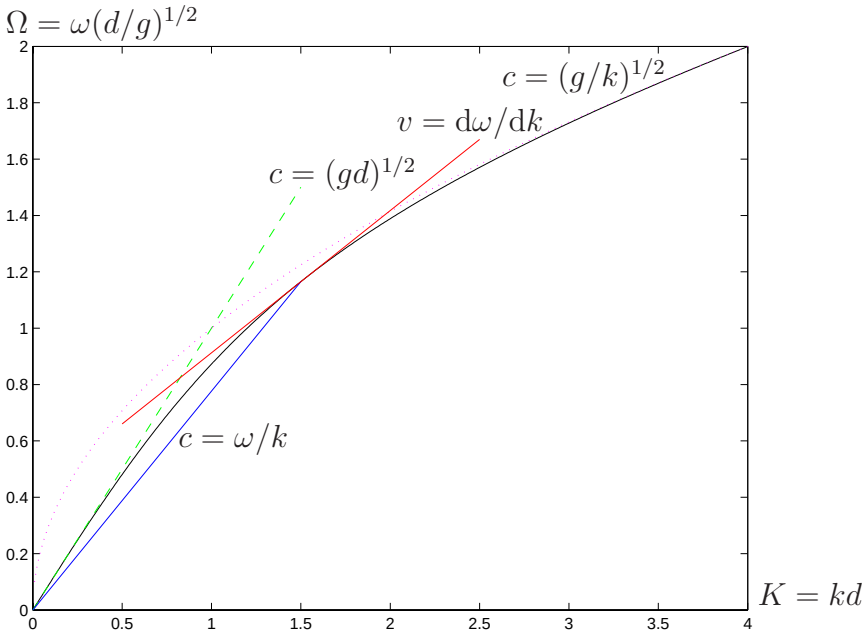

Fig. 8-I. The dispersion curve for gravity water waves, with the short and long wavelength limits illustrated, and the derivation of the phase c and group v velocity from this curve.

returning from Sri Lanka in the immediate aftermath of the Asian tsunami disaster of 26 December 2004.

In terms of a dimensionless frequency, $\Omega = \omega(d/g)^{1/2}$, where d is the water depth and g the acceleration due to gravity, and dimensionless wavenumber, $K = kd$, the dispersion relation for gravity water waves on a flat ocean is

$$\Omega^2 = K \tanh K.$$

This gives dimensionless phase and group velocities of

$$\begin{aligned} C &= c(gd)^{-1/2} = \frac{\Omega}{K} = \left(\frac{\tanh K}{K}\right)^{1/2} \\ V &= v(gd)^{-1/2} = \frac{\mathrm{d}\Omega}{\mathrm{d}K} = \frac{\tanh K + K\mathrm{sech}^2 K}{2\Omega}, \end{aligned}$$

respectively. The dispersion curves for these functions is shown in the Figures 8-I and 8-II.

In fact for tsunami, we only need the long-wavelength limit, $K \ll 1$, when the phase and group velocities can be approximated by the quadratic

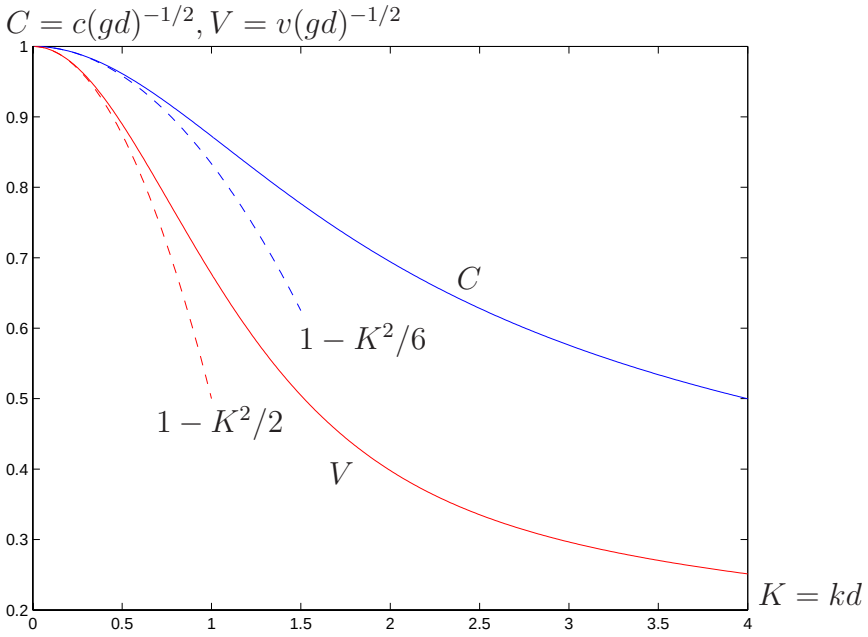

Fig. 8-II. The phase and group velocities for gravity water waves, derived from the dispersion curve in Figure 8-I, with the long-wavelength approximations indicated.

term, i.e. for dimensionless velocities, these are

$$\begin{aligned} C &\simeq 1 - K^2/6 \\ V &\simeq 1 - K^2/2, \end{aligned}$$

respectively. Then a wavenumber integral can be evaluated using the Airy function (D.2.9) to give the wave displacement in the form of the so-called Jeffreys phase (Bullen and Bolt, 1963, p. 465)†

$$\begin{aligned} u &= \int_{-\infty}^{\infty} \mathrm{e}^{\mathrm{i}(\Omega T - KX)} \mathrm{d}K \simeq \int_{-\infty}^{\infty} \mathrm{e}^{\mathrm{i}K(T-X) - \mathrm{i}K^3 T/6} \mathrm{d}K \\ &= \frac{2\pi}{(T/2)^{1/3}} \, Ai\left(\frac{X - T}{(T/2)^{1/3}} \right), \end{aligned}$$

where $T = t(g/d)^{1/2}$ is the dimensionless time variable, and $X = x/d$ the dimensionless range. For realistic values for the propagation to Sri Lanka of $d = 5$ km and $x = 2000$ km, this gives $X = 400$. The limiting phase and group velocities are $C = V = 1$ or $c = v = 220$ m/s, giving

† Bullen, K.E. and Bolt, B.A., 1985. *An Introduction to the Theory of Seismology*, 4th edn, Cambridge: Cambridge University Press

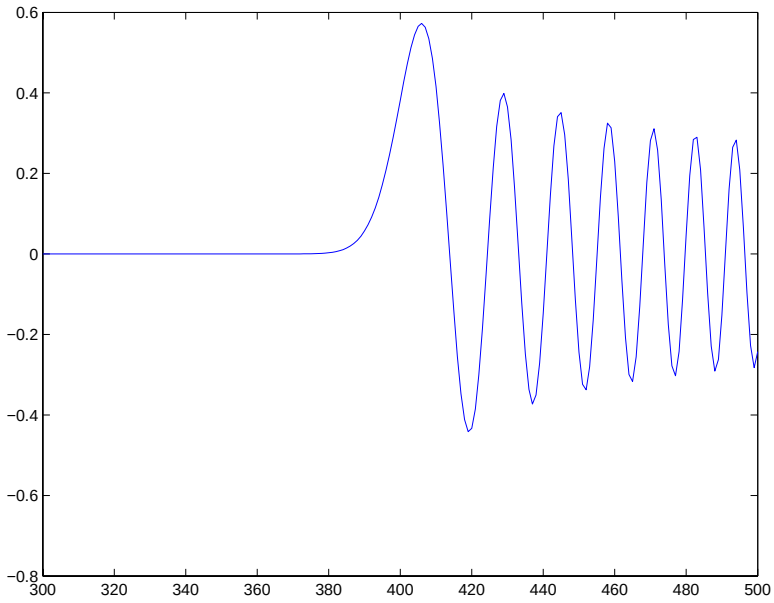

Fig. 8-III. The Jeffreys phase for $X = 400$.

an arrival time of $T = 400$ or $t = 9000$ s $= 150$ mins. A dimensional time unit is 22.5 s, or 1 hour equals 160 units. Figure 8-III illustrates the Jeffreys phase at this range. The important features of the Jeffreys phase, caused by the stationarity of the velocity with respect to wavenumber and frequency, are the slow decay with range, $X^{-1/3}$, due to dispersion (this is the decay due to second-order dispersion only, i.e. one-dimensional wave propagation. Including the geometrical spreading in two dimensions, the decay rate would be increased to $X^{-5/6}$), the build up to an initial, large wave and the slow amplitude decay and decreasing periods at later times.

Although the general form of this waveform corresponds to observations in Sri Lanka, a major discrepancy exists in the period of the oscillations. A small precursor wave observed could probably be modelled easily by including a phase shift in the wavenumber integral. Periods of about 20 dimensionless units correspond to 7.5 mins, whereas observed periods were significantly longer, e.g. 45 mins. This must have been caused by the earthquake's mechanism, large magnitude ($M = 9$ on the Richter scale) and dimensions. Normally when a source propagates towards the observer, the Doppler shift increases the frequency (decreases the pulse width),

e.g. for a seismic waveforms. But the rupture velocity is supersonic with respect to the tsunami velocity (2000 m/s compared with 220 m/s), so the effect is different. Effectively an observer in Sri Lanka, in the direction of the rupture propagation, sees tsunami waves from the last point of rupture (the nearest point) first, and from the first point of rupture (the furthest point) last. In fact the rupture velocity is so high (as it is in rock), about ten times the tsunami velocity, that the direction of rupture relative to the observation point is not very important. The tsunami from the nearest point of rupture always arrives first, and from the furthest last. For simple numerical calculations, we can assume that all the rupture occurs instantaneously, i.e. an infinite rupture velocity. The pulse can be broadened by the interference of waves generated all along the rupture. This can be simulated by integrating the Jeffreys phase

$$u = \frac{2\pi}{(T/2)^{1/3}} \int w(x)\, Ai\left(\frac{x-T}{(T/2)^{1/3}}\right) \mathrm{d}x,$$

where $w(x)$ is a weighting function indicating the source strength along the rupture. Numerical experiments show that the resultant waveforms are very sensitive to the width and form of this weighting function. Trials have been made with triangular and boxcar weights of various widths. If the weighting function is narrow (a few dimensionless units) the wave shape is close to the Jeffreys phase, of course. With a greater width (say 20 units), the main change is that waves from the two ends of the rupture of slightly different frequencies (because the frequencies in the Jeffreys phase increase with propagation time), interfere and cause beats and a more rapid decay. For long source widths (40 units and greater), the wave begins to have approximately the form of the weighting function with reduced later oscillations (for large integration lengths, the Airy function in the above integral looks more like a Dirac delta function). In reality, it is unlikely that the high-frequency oscillations in the interference beats will propagated coherently due to spatial variations of the source and ocean. If these oscillations are removed, the remaining long-period oscillations from the amplitude of the beats begin to approximate the observations better. Although these numerical simulations are instructive, further numerical experiments with such a simple model seem pointless given the sensitivity of the final waveform to the source weighting function, and the undoubted complexity of such a large earthquake. The varying water depth of the actual ocean will cause further dispersion and focusing of energy. Full

numerical simulations for realistic models of tsunami propagation are calculated routinely.

- *Page 456:* **Erratum** — in the caption to Figure 9.38 (page 456), a minus sign is missing in the exponent. It should read "The waveforms in the deep shadow given by approximation $(V_1\ell_1)^{-11/2}Sh^{(3)}\left(3(V_1\ell_1)^{-3}(t-\widetilde{T}_1)\right)$ (9.3.101) with $V_1 = 1$. The time axis is the reduced travel time, $\overline{t} = t - \widetilde{T}_1$, and the range axis is the reduced range, $\overline{X} = \ell_1 = x_{\mathsf{R}} - X_1$."

- *Pages 478 and 480:* **Erratum** — on page 478 and in the caption to Figure 10.11 (page 480), the receiver coordinate should be $y_{\mathsf{R}} = 0.05$ km (not $y_{\mathsf{R}} = 0.005$ km).

- *Pages 490 to 494:* **Erratum** — in equations (10.2.7), (10.2.18), (10.2.31), (10.2.32) and (10.2.33), and in the text following the last equation, the symbol B_{MN} should not have a suffix ^{0}.

- *Equation (10.2.8) and pages 490 to 503:* **Revision** — in defining B_{MN} in equation (10.2.8) and all the following usage it would have been more consistent to use the symbol ΔB_{MN} and to expand equation (10.2.8) to read

$$\Delta B_{MN} = \Delta B(\hat{\mathbf{g}}_M, \hat{\mathbf{g}}_N) = \hat{p}_j \hat{p}_k \, \hat{\mathbf{g}}_M^{\mathrm{T}} \, \Delta\mathbf{a}_{jk} \, \hat{\mathbf{g}}_N. \qquad (10.2.8)$$

- *Pages 492–4, equations (10.2.21), (10.2.22), (10.2.27), (10.2.28) and (10.2.33):* **Erratum** — The text and equations (10.2.21) and (10.2.22) are confused and should read (we have revised the notation as suggested above):

  Substituting in the perturbation equation (10.2.3) with $I = 1$, we can pre-multiply by $\hat{\mathbf{e}}_1^{0^{\mathrm{T}}}$ or $\hat{\mathbf{e}}_2^{0^{\mathrm{T}}}$ to obtain two simultaneous equations

$$\begin{aligned} \cos\phi\,(2c^0\Delta c_1 - \Delta B_{11}) - \sin\phi\,\Delta B_{12} &= 0 \qquad (10.2.21) \\ -\cos\phi\,\Delta B_{21} + \sin\phi\,(2c^0\Delta c_1 - \Delta B_{22}) &= 0, \qquad (10.2.22) \end{aligned}$$

  and similarly for $I = 2$, where again we have taken the phase direction, $\hat{\mathbf{p}}$, fixed and the elements $\Delta B_{\eta\nu}$ are defined using the vectors $\hat{\mathbf{e}}_\eta^0$, i.e. $\Delta B_{\eta\nu} = \Delta B(\hat{\mathbf{e}}_M^0, \hat{\mathbf{e}}_N^0)$.

  In order that in the rotated system

$$\Delta\mathbf{b} = \Delta\widetilde{\mathbf{B}} = \begin{pmatrix} \Delta b_1 & 0 \\ 0 & \Delta b_2 \end{pmatrix} = \mathbf{\Phi}^{-1}\Delta\mathbf{B}\mathbf{\Phi}$$

(see equations (10.2.26) and (10.2.55)), $\Delta b_1 < \Delta b_2$ as required (as in equation (10.2.24)), the alternative solution of equation (10.2.29) should be taken, i.e.

$$\sin\phi = \frac{1}{\sqrt{2}}\left(1+\frac{\Delta B_{11}-\Delta B_{22}}{B}\right)^{1/2} \tag{10.2.27}$$

$$\cos\phi = -\frac{\mathrm{sgn}(\Delta B_{12})}{\sqrt{2}}\left(1-\frac{\Delta B_{11}-\Delta B_{22}}{B}\right)^{1/2}. \tag{10.2.28}$$

Some subscripts in equation (10.2.33) are in error. The correct form is

$$\begin{aligned} g_{12} &= \frac{\Delta\ B_{13}\ \Delta\ B_{23}}{(\ \Delta\ B_{11}\ -\ \Delta\ B_{22}\ )\left(c_1^{0\,2}-c_3^{0\,2}\right)} \\ &= \frac{\Delta B_{13}\Delta B_{23}}{2c^0\,(\Delta c_1-\Delta c_2)\left(c_1^{0\,2}-c_3^{0\,2}\right)}, \end{aligned} \tag{10.2.33}$$

giving the first-order perturbation to the polarization provided $\Delta\ B_{11} \neq \Delta\ B_{22}$, i.e. provided the anisotropy removes the degeneracy $\Delta c_1 \neq \Delta c_2$.

- *Page 515, equations (10.3.46) and (10.3.47):* **Erratum** — The symbol Λ should be Φ so the equations are

$$\underline{\mathbf{F}}^{\mathrm{A}}(\omega,\mathbf{x};\mathbf{x}_{\mathsf{S}}) = -f^{(\ell)}(\omega)\ \Phi\,(\omega,\mathbf{x},\mathcal{L}_{\mathsf{S}})\,\nabla\underline{P}^{(0)}(\mathbf{x},\mathcal{L}_{\mathsf{S}}) \tag{10.3.46}$$

$$\underline{\Theta}^{\mathrm{A}}(\omega,\mathbf{x};\mathbf{x}_{\mathsf{S}}) = -\frac{1}{\mathrm{i}\,\omega}f^{(\ell)}(\omega)\ \Phi\,(\omega,\mathbf{x},\mathcal{L}_{\mathsf{S}})\,\nabla\cdot\underline{\mathbf{v}}^{(0)}(\mathbf{x},\mathcal{L}_{\mathsf{S}}) \tag{10.3.47}$$

- *Page 521:* **Erratum** — equation (10.3.70) contains a sign error. It should read

$$\underline{\boldsymbol{\mathcal{K}}}^{\mathrm{B}}(\mathbf{x},\mathcal{L}_{\mathsf{R}},\mathcal{L}_{\mathsf{S}}) = \underline{\mathbf{v}}^{(0)\,\mathrm{T}}(\mathbf{x},\mathcal{L}_{\mathsf{R}})\,\rho^{\mathrm{B}}(\mathbf{x})\,\underline{\mathbf{v}}^{(0)}(\mathbf{x},\mathcal{L}_{\mathsf{S}}) - \underline{P}^{(0)\,\mathrm{T}}(\mathbf{x},\mathcal{L}_{\mathsf{R}})\,k^{\mathrm{B}}(\mathbf{x})\,\underline{P}^{(0)}(\mathbf{x},\mathcal{L}_{\mathsf{S}}). \tag{10.3.70}$$

The error does not persist and equation (10.3.72) is correct.

- *Page 522:* **Erratum** — the time derivative in equation (10.3.75) should be second derivatives. The equation should read

$$\underline{\mathbf{u}}^{\mathrm{B}}(t,\mathbf{x}_{\mathsf{R}};\mathbf{x}_{\mathsf{S}}) = -\frac{1}{4\pi^2}\frac{\mathrm{d}^{\,2}}{\mathrm{d}t^{\,2}}\int_V \mathrm{Re}\left(\underline{\boldsymbol{\mathcal{K}}}^{\mathrm{B}}(\mathbf{x},\mathcal{L}_{\mathsf{R}},\mathcal{L}_{\mathsf{S}})\,\Delta\left(t-\widetilde{T}(\mathbf{x},\mathcal{L}_{\mathsf{R}},\mathcal{L}_{\mathsf{S}})\right)\right)\mathrm{d}V. \tag{10.3.75}$$

Equation (10.3.76) was correct.

- *Pages 530:* **Erratum** — equation (10.3.88) contained a sign error. It should read

$$\Gamma^{\mathrm{B}}(\mathbf{x}, \mathcal{L}_{\mathsf{R}}, \mathcal{L}_{\mathsf{S}}) \simeq \frac{\alpha^{\mathrm{B}}}{\alpha^2} \,. \tag{10.3.88}$$

  Equation (10.3.89) was correct.

- *Pages 551:* **Appendum** — add an extra exercise:

  Exercise 10.7 Show that expression (10.3.55) for the acoustic Born error term can be reduced to

$$\Gamma^{\mathrm{E}}(\mathbf{x}, \mathcal{L}_{\mathsf{R}}, \mathcal{L}_{\mathsf{S}}) = \frac{1}{4}\left(\hat{\mathbf{g}}(\mathbf{x}, \mathcal{L}_{\mathsf{R}}) + \hat{\mathbf{g}}(\mathbf{x}, \mathcal{L}_{\mathsf{S}})\right) \cdot \nabla \ln \left(Z(\mathbf{x})\mathcal{T}^{(\ell)}(\mathbf{x}, \mathcal{L}_{\mathsf{R}})\mathcal{T}^{(\ell)}(\mathbf{x}, \mathcal{L}_{\mathsf{S}})\right) .$$

  Answer: The scalar Born error acoustic scattering term contains the divergence of the normalized polarizations, $\hat{\mathbf{g}}$, and the gradient of the ray scalar amplitude, $\mathcal{T}$ (5.4.34). These are related.

  Poynting's vector (5.2.6) gives

$$\nabla \cdot \left(P^{(0)}\mathbf{v}^{(0)}\right) = 0,$$

  and substituting for the ray dyadic (5.4.31) with (5.4.33) this reduces to

$$\nabla \cdot \left(\mathcal{T}^2 \hat{\mathbf{g}}\right) = 0,$$

  assuming the source terms are isotropic. As a check, let us expand giving

$$\begin{aligned} \nabla \cdot \hat{\mathbf{g}} &= -\hat{\mathbf{g}} \cdot \nabla(\ln \mathcal{T}^2) \\ &= \hat{\mathbf{g}} \cdot \nabla(\ln \mathcal{R}^2) \\ &= \hat{\mathbf{g}} \cdot \nabla(\ln J). \end{aligned}$$

  as the scalar ray amplitude is inversely proportional to the effective ray length, $\mathcal{R}$ (5.4.34) with (5.2.72), and inversely proportional to the square root of the ray tube cross-section, J (5.2.13) (the impedance factor Z in equation (5.2.13) is part of the receiver normalization in $\mathbf{g}$, (5.4.31) with (5.4.33), not the transmission term, $\mathcal{T}$ (5.4.34)). These results are consistent with those in Exercise 5.5

$$\nabla \cdot \hat{\mathbf{p}} = K,$$

  and

$$\frac{\mathrm{d}J}{\mathrm{d}s} = JK,$$

where K is the wavefront curvature, i.e.

$$\nabla \cdot \hat{\mathbf{g}} = K = \frac{\mathrm{d}}{\mathrm{d}s}(\ln J) = \hat{\mathbf{g}} \cdot \nabla(\ln J).$$

They are easily checked for a spherical wavefront in a homogeneous medium with $\mathcal{R} = r$, $\hat{\mathbf{g}} = \hat{\mathbf{r}}$, $K = 2/r$ and $\nabla \cdot \hat{\mathbf{r}} = 2/r$.

The scalar Born error acoustic scattering term (10.3.55) is

$$\Gamma^{\mathrm{E}} = \frac{1}{4}\left(\nabla \ln Z - \nabla\right) \cdot (\hat{\mathbf{g}}^{\mathsf{R}} + \hat{\mathbf{g}}^{\mathsf{S}}) - \frac{1}{4}\left(\nabla \ln \frac{\mathcal{T}^{\mathsf{R}}}{\mathcal{T}^{\mathsf{S}}}\right) \cdot (\hat{\mathbf{g}}^{\mathsf{R}} - \hat{\mathbf{g}}^{\mathsf{S}}).$$

For brevity, we omit the arguments and indicate the source/receiver rays by a superscript, i.e. $\mathbf{g}(\mathbf{x}, \mathcal{L}_{\mathsf{S}}) = \mathbf{g}^{\mathsf{S}}$. Substituting for the divergence of the polarization, this reduces to

$$\Gamma^{\mathrm{E}} = \frac{1}{4}(\hat{\mathbf{g}}^{\mathsf{R}} + \hat{\mathbf{g}}^{\mathsf{S}}) \cdot \nabla \ln(Z\,\mathcal{T}^{\mathsf{R}}\mathcal{T}^{\mathsf{S}}),$$

the required elegant, symmetric result.

- *Pages 551:* **Appendum** — add an extra exercise:

Exercise 10.8 Show that expression (10.3.78) can be reduced to

$$\Gamma^{\mathrm{B}}(\mathbf{x}, \mathcal{L}_{\mathsf{R}}, \mathcal{L}_{\mathsf{S}}) = \mathbf{g}^{\mathrm{T}}(\mathbf{x}, \mathcal{L}_{\mathsf{R}})\, \rho^{\mathrm{B}}(\mathbf{x})\, \mathbf{g}(\mathbf{x}, \mathcal{L}_{\mathsf{S}}) + \mathbf{\Theta}^{\mathrm{T}}(\mathbf{x}, \mathcal{L}_{\mathsf{R}}) : \mathbf{c}^{\mathrm{B}}(\mathbf{x}) : \mathbf{\Theta}(\mathbf{x}, \mathcal{L}_{\mathsf{S}}),$$

where

$$\mathbf{\Theta}^{\mathrm{T}}(\mathbf{x}, \mathcal{L}) = \frac{1}{2}\left(\mathbf{p}(\mathbf{x}, \mathcal{L})\mathbf{g}^{\mathrm{T}}(\mathbf{x}, \mathcal{L}) + \mathbf{g}(\mathbf{x}, \mathcal{L})\mathbf{p}^{\mathrm{T}}(\mathbf{x}, \mathcal{L})\right),$$

is a symmetric dyadic formed from the ray slowness and energy-normalized polarization, and the shorthand notation (:) indicates contraction of the fourth-order stiffness perturbation tensor with the dyadic of the source and receiver rays.

Answer: The first term involving the density perturbation is identical, so we only consider the second term. For brevity, we omit the arguments and indicate the source/receiver rays by a superscript, i.e. $\mathbf{g}(\mathbf{x}, \mathcal{L}_{\mathsf{S}}) = \mathbf{g}^{\mathsf{S}}$. Using subscript notation, the scalar of interest is

$$\begin{aligned} -\,\mathbf{g}^{\mathsf{R}^{\mathrm{T}}}\mathbf{Z}_k^{\mathsf{R}^{\mathrm{T}}}\mathbf{s}_{kj}^{\mathrm{B}}\mathbf{Z}_j^{\mathsf{S}}\mathbf{g}^{\mathsf{S}} &= -\,g_a^{\mathsf{R}}\left(\mathbf{Z}_k^{\mathsf{R}}\right)_{ba}\left(\mathbf{s}_{kj}^{\mathrm{B}}\right)_{bc}\left(\mathbf{Z}_j^{\mathsf{S}}\right)_{cd} g_d^{\mathsf{S}} \\ &= -\,g_a^{\mathsf{R}}(p_m^{\mathsf{R}} c_{ambk}) s_{bkcj}^{\mathrm{B}} (p_l^{\mathsf{S}} c_{cjdl}) g_d^{\mathsf{S}} \\ &= -\,(g_a p_m)^{\mathsf{R}} (p_l g_d)^{\mathsf{S}} (c_{ambk}\, s_{bkcj}^{\mathrm{B}}\, c_{cjdl}), \end{aligned}$$

where, of course, we have assumed the Einstein summation convention

over the repeated indices j and k, and a, b, c and d, and used definitions (5.3.22) and (4.4.37).

We denote the second-order, symmetric tensor by $\mathbf{\Theta}$ where

$$\Theta_{ij} = \frac{1}{2}(g_i p_j + g_j p_i) \quad \text{or} \quad \mathbf{\Theta} = \frac{1}{2}(\mathbf{g}\,\mathbf{p}^{\mathrm{T}} + \mathbf{p}\,\mathbf{g}^{\mathrm{T}})$$

(this symbol is used as overwriting g and p looks like θ, and its trace is related to the dilatation (4.2.8)).

Differentiating expression (4.4.43), we have

$$c^{\mathrm{B}}_{ijpq} s_{pqrs} + c_{ijpq} s^{\mathrm{B}}_{pqrs} = 0,$$

to first-order. Thus

$$\begin{aligned} c_{ambk} s^{\mathrm{B}}_{bkcj} c_{cjdl} &= -\, c^{\mathrm{B}}_{ambk} s_{bkcj} c_{cjdl} \\ &= -\, c^{\mathrm{B}}_{ambk} \frac{1}{2}\,(\delta_{bd}\delta_{kl} + \delta_{bl}\delta_{kd}) \\ &= -\, c^{\mathrm{B}}_{amdl}, \end{aligned}$$

using expression (4.4.43) and symmetries again. Thus the term of interest is

$$\begin{aligned} -\,\mathbf{g}^{\mathsf{R}^{\mathrm{T}}} \mathbf{Z}^{\mathsf{R}^{\mathrm{T}}}_k \mathbf{s}^{\mathrm{B}}_{kj} \mathbf{Z}^{\mathsf{S}}_j \mathbf{g}^{\mathsf{S}} &= \Theta^{\mathsf{R}}_{am} c^{\mathrm{B}}_{amdl} \Theta^{\mathsf{S}}_{dl} \\ &= \mathbf{\Theta}^{\mathsf{R}} : \mathbf{c}^{\mathrm{B}} : \mathbf{\Theta}^{\mathsf{S}}, \end{aligned}$$

using the shorthand notation. With this expression, we can easily obtain the special forms in isotropic and TIV media.

The early publications on the Born approximation in elastic media (Bhatia, 1959†; Miles, 1960‡) only discussed isotropic media. Hudson and Heritage (1981) gave the general anisotropic result, and substituting the ray Green function in their equation (3) would reduce to the above result. Ben-Menahem and Gibson (1990) considered TIV media and Gibson and Ben-Menahem (1991) generalized this. More recently, Burridge, de Hoop, Miller and Spencer (1998) have given an expression very similar to ours, i.e. their equation (3.28) with the dyadics (3.25) and (3.26).

- *Page 597:* **Erratum** — on page 597 in the Bibliography, the page numbers for Thomson and Chapman (1984) should be 385–410 .

† Bhatia, A.B., 1959. Scattering of high-frequency sound waves in polycrystalline materials, *J. Acoust. Soc. Amer.*, **31**, 16–23.

‡ Miles, J.W., 1960. Scattering of elastic waves by small inhomogeneities, *Geophysics*, **25**, 642–8.

- *Pages 602 and 604:* **Erratum** — "Bessel function" and "Hankel function" should have references to Appendix B.4, i.e. 562–563.

- *Page 608:* **Erratum** — the item "tranversely isotropic medium, 232" should obviously have been included in the previous line for "transversely isotropic medium".